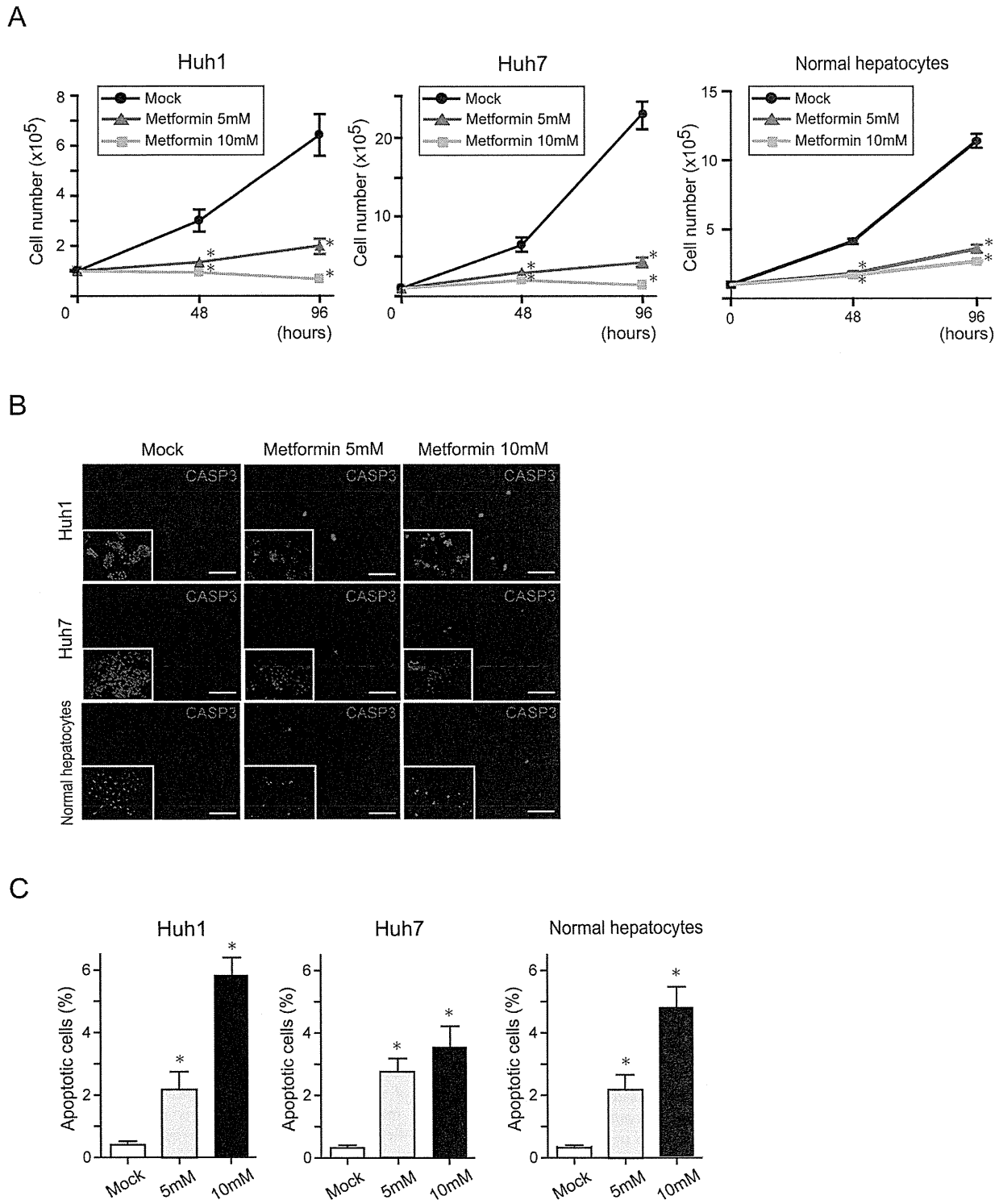

Figure 1. *In vitro* assays of HCC cells and normal hepatocytes treated with metformin. (A) Dose-dependent and time-dependent inhibition of the growth of HCC cells and normal hepatocytes treated with metformin. *Statistically significant ($p<0.05$). (B) Detection of apoptotic cells by immunostaining of CASP3. Nuclear DAPI staining is shown in the insets. Scale bar = 100 μm. (C) Quantification of the percentage of apoptotic cells. *Statistically significant ($p<0.05$).
doi:10.1371/journal.pone.0070010.g001

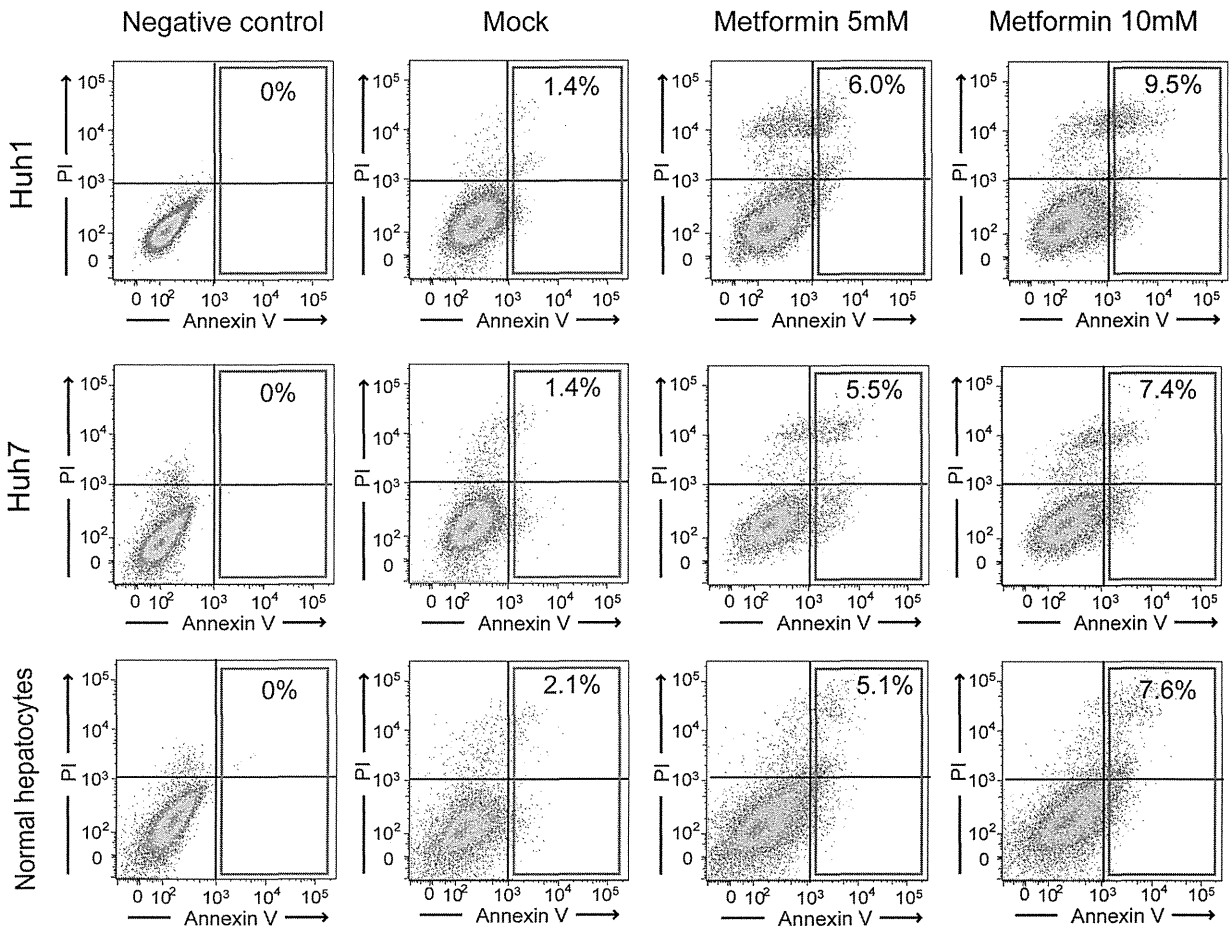

Figure 2. Detection of apoptotic cells by staining with Annexin V and PI using flow cytometry. The percentages of Annexin V-positive cells are shown as the mean values for three independent analyses.
doi:10.1371/journal.pone.0070010.g002

sorafenib (Fig. 7C). Co-treatment with metformin and sorafenib produced results similar to the single administration of metformin (Fig. 7C).

Re-analysis of Subcutaneous Tumors

Consistent with the pathological findings, flow cytometric analysis of xenograft tumors clearly demonstrated that metformin markedly reduced the number of tumor-initiating $EpCAM^+$ cells, whereas sorafenib did not (Fig. 8A). We conducted the non-adherent sphere formation assay of $EpCAM^+$ cells isolated from subcutaneous tumors. Metformin treatment as well as co-treatment with sorafenib markedly impaired primary sphere formation and even more severely impaired secondary sphere formation (Fig. 8B and 8C). In contrast, sorafenib treatment had very little effect on the formation of primary and secondary spheres (Fig. 8B and 8C). Taken together, metformin could be a therapeutic agent for the elimination of tumor-initiating HCC cells, at least in part by inhibiting their self-renewal capacity.

Discussion

A large number of studies have suggested that metformin has an anti-cancer effect in various types of malignancies including breast cancer and ovarian cancer, and even in HCC [14–16]. However, its efficacy against tumor-initiating HCC cells remains to be elucidated.

In this study, we first conducted cell growth assays in non-purified Huh1 and Huh7 cells treated with metformin. Consistent with previous reports, metformin treatment inhibited cell growth and induced apoptosis in both cell lines in dose-dependent and time-dependent manners. In addition, flow cytometric analysis showed a decrease in the proportion of $EpCAM^+$ and $CD133^+$ cells. These results prompted us to examine the direct action of metformin against tumor-initiating HCC cells. Sphere formation assays showed that metformin significantly suppressed the formation of spheres generated from $EpCAM^+$ TICs in a dose-dependent manner. Subsequent analysis for secondary sphere formation after replating showed similar results to those of primary sphere assays. In addition, immunocytochemical analysis revealed that metformin treatment reduced the number of $EpCAM^+$ and AFP^+ cells in primary spheres. Taken together, it appears that metformin impaired $EpCAM^+$ tumor-initiating HCC cells and simultaneously promoted the differentiation towards non-TICs.

Dependency on the mTOR pathway was shown to be higher in leukemic stem cells (LSCs) than in normal hematopoietic stem cells and the mTOR inhibitor rapamycin impaired the self-renewal of LSCs in leukemic mouse models [18]. mTOR signaling also makes a significant contribution to the maintenance of TICs in breast

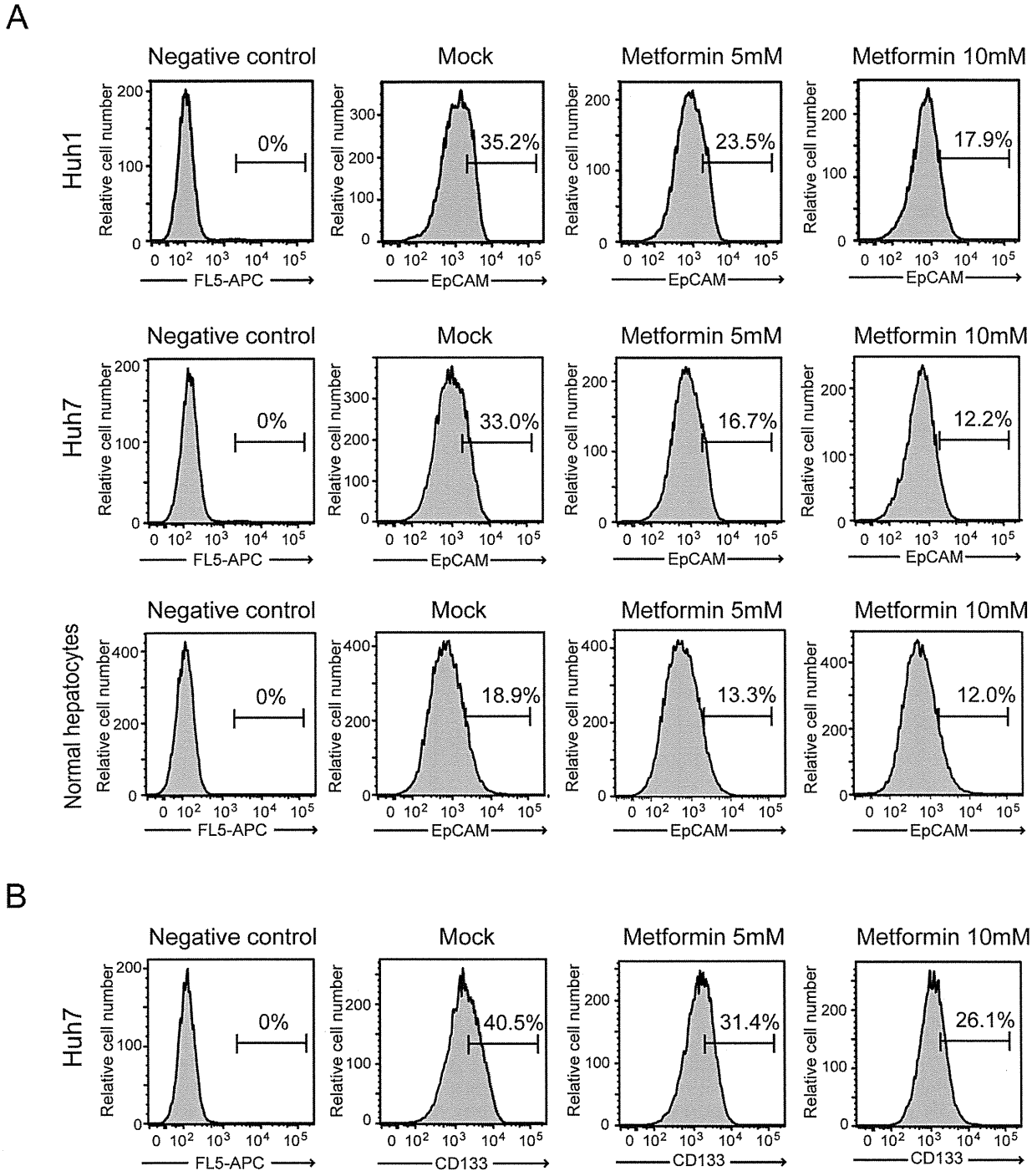

Figure 3. Flow cytometric profiles of HCC cells and normal hepatocytes treated with metformin (5 or 10 mM) for 72 hours. (A) The percentages of $EpCAM^+$ fractions are shown as the mean values for three independent analyses. (B) The percentages of $CD133^+$ fractions in Huh7 cells are shown as the mean values for three independent analyses.
doi:10.1371/journal.pone.0070010.g003

cancer and prostate cancer [19,20]. The aberrant activation of mTOR signaling was also observed in approximately 50% of patients with HCC [21,22]. The mTOR inhibitor, everolimus, which is currently undergoing clinical trials, exhibited an anti-tumor effect in some cases of advanced HCC [23]. Taken together, it appears that mTOR signaling plays an important role in hepatocarcinogenesis and the progression of HCC.

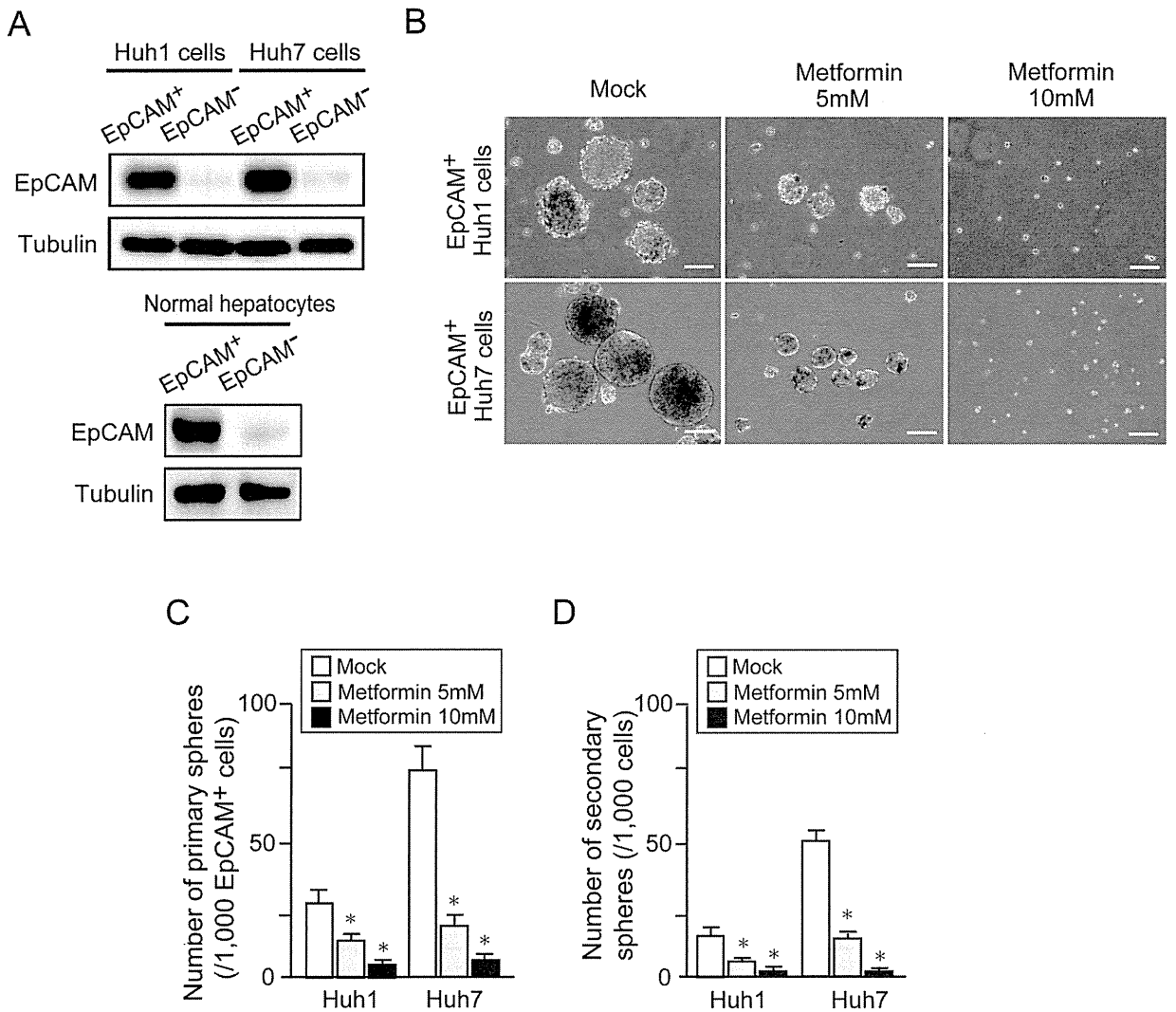

Figure 4. Non-adherent sphere formation assays of EpCAM$^+$ cells treated with metformin. (A) Western blot analysis of EpCAM expression in sorted EpCAM$^+$ cells. Tubulin was used as a loading control. (B) Bright-field images of the non-adherent spheres of EpCAM$^+$ HCC cells at day 14 of culture. Scale bar = 100 μm. (C) Number of large spheres generated from 1,000 EpCAM$^+$ cells treated with metformin. *Statistically significant ($p<0.05$). (D) Number of secondary spheres 14 days after replating. *Statistically significant ($p<0.05$).
doi:10.1371/journal.pone.0070010.g004

In the present study, metformin treatment apparently inhibited the mTOR pathway by phosphorylating AMPK in EpCAM$^+$ Huh7 cells. Considering that mTOR inhibitors suppressed the growth of Huh7 cells not only in culture but also in xenograft models [24,25], it is assumed that metformin exerted its anti-TIC effect by affecting the AMPK/mTOR pathway. In contrast, metformin did not alter the activity of the mTOR pathway in EpCAM$^+$ Huh1 cells despite inducing the phosphorylation of AMPK. One possible explanation for this is that mutations in the components of the mTOR pathway, which have been identified in many cancers and cancer cell lines, mask the effect of metformin in EpCAM$^+$ Huh1 cells [26]. Another possibility is that the mTOR pathway is not the major target of metformin and anti-tumor activity is exerted independent of the pathway. Several reports support this notion. For example, metformin was shown to cause cell cycle arrest by downregulating the expression of cyclin D1 and/or upregulating that of cyclin-dependent kinase inhibitors such as $p21^{Cip1}$ without inhibiting the mTOR pathway [27,28]. A previous report also attributed the anti-tumor activity of metformin to NF-kB inhibition in breast CSCs [29]. In addition, a recent study revealed a novel mechanism whereby metformin blocked glucagon-dependent glucose output from hepatocytes by reducing cyclic AMP and protein kinase A levels [30]. In the present study, metformin treatment suppressed the expression of cyclin D1 in EpCAM$^+$ HCC cells, but not in EpCAM$^+$ normal hepatcytes. Conversely, metformin increased p21 expression in EpCAM$^+$ normal hepatcytes, but not in EpCAM$^+$ HCC cells. Further analyses on the mechanisms of the anti-TIC activity of metformin are required.

Sorafenib is the sole molecular target drug clinically approved to treat advanced HCC. However, phase III trials have shown

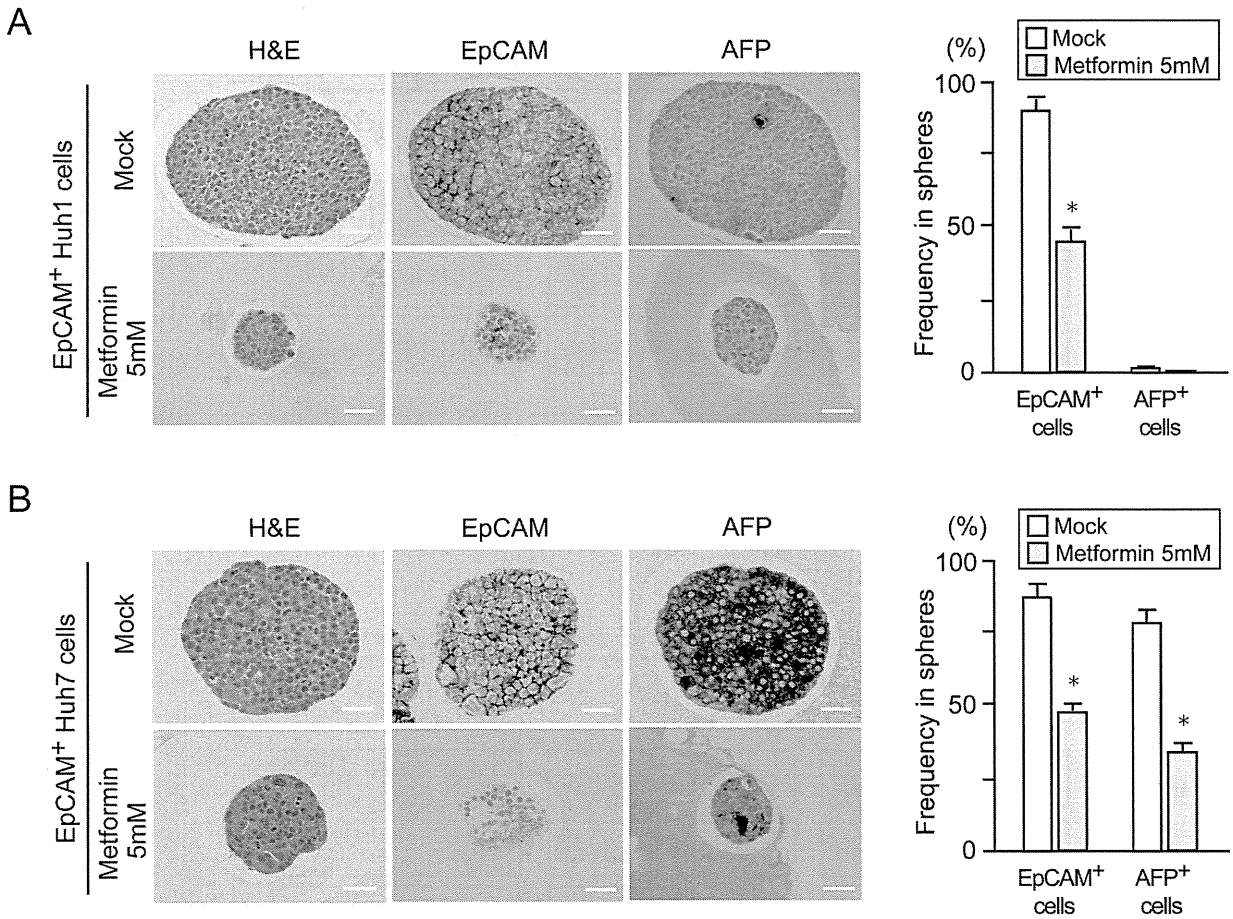

Figure 5. Immunostaining of EpCAM$^+$ cell-derived spheres. (A) Hematoxylin and eosin staining and immunocytochemical analysis of EpCAM and AFP in spheres derived from EpCAM$^+$ cells. Scale bar = 20 μm. (B) The percentage of EpCAM$^+$ cells or AFP$^+$ cells was determined. *, Statistically significant ($p<0.05$).
doi:10.1371/journal.pone.0070010.g005

that sorafenib prolonged median overall survival of patients with advanced HCC by no more than 3 months [31,32]. In our xenograft transplantation assay, treatment with metformin and sorafenib similarly suppressed the growth of subcutaneous tumors and co-treatment appeared to be more effective. Interestingly, both flow cytometric analysis and immunohistochemical analysis of xenograft tumors revealed that metformin significantly reduced the number of tumor-initiating EpCAM$^+$ cells, whereas sorafenib treatment had minimal effects on TICs. Taking these results into consideration, it is possible that the combined use of metformin and sorafenib exhibited stronger anti-tumor effect than sorafenib treatment alone in HCC.

In summary, metformin reduced the number and tumorigenicity of tumor-initiating HCC cells; however the involvement of the AMPK/mTOR pathway in its anti-tumor activity remains ambiguous. Because metformin suppressed cell growth and decreased the number of EpCAM$^+$ normal hepatocytes, further analysis might be necessary to determine whether metformin affects the function of normal hepatic stem/progenitor cells [33]. It is of importance to examine whether metformin might be of use for the elimination of TICs in HCC in clinical trials.

Materials and Methods

Ethics Statement

All experiments using mice were performed in accordance with our institutional guidelines for the use of laboratory animals and approved by the Review Board for Animal Experiments of Chiba University (approval ID: 22–187).

Mice and Reagents

NOD/SCID mice (Sankyo Laboratory Co. Ltd., Tsukuba, Japan) were bred and maintained in accordance with our institutional guidelines for the use of laboratory animals (approval ID: 22–187). Metformin (1,1-dimethylbiguanide hydrochloride) and sorafenib tosylate were purchased from Sigma-Aldrich (St. Louis, MO) and LKT laboratories (Saint Paul, MN), respectively.

Cell Culture and Sphere Formation Assay

The HCC cell lines, Huh1 and Huh7, were obtained from the Health Science Research Resources Bank (HSRRB, Osaka, Japan). Normal human hepatocytes were obtained from ACBRI (Kirkland, WA, USA). Cells were cultured in Dulbecco's modified Eagle's medium (Invitrogen Life Technologies, Carlsbad, CA) containing 10% fetal calf serum and 1% penicillin/streptomycin

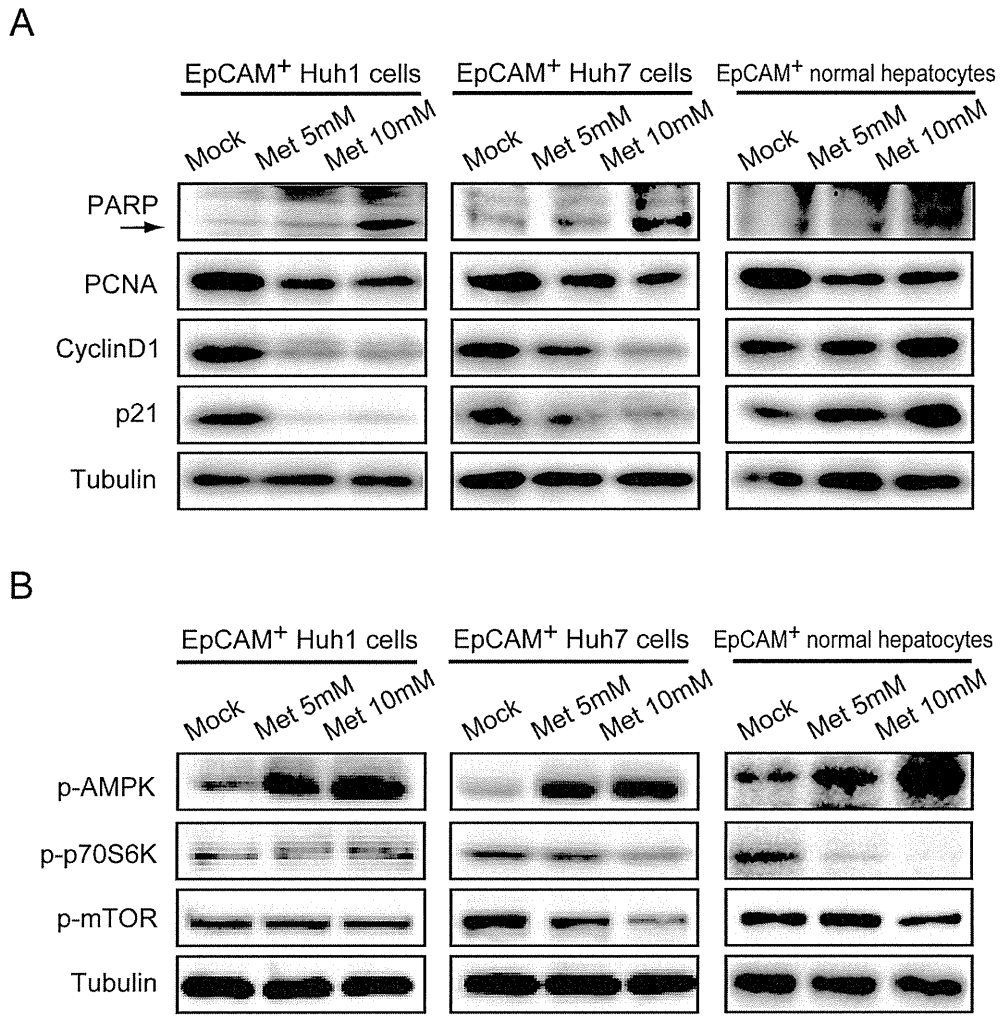

Figure 6. Cell growth inhibition, induction of apoptosis, and inhibition of the mTOR pathway after metformin treatment in HCC cells and normal hepatocytes. (A) EpCAM$^+$ cells were subjected to Western blot analysis using anti-PARP, PCNA, cyclin D1, p21, and tubulin (loading control) antibodies. The arrow indicates the cleaved forms of PARP. (B) EpCAM$^+$ cells were subjected to Western blotting using anti-phospho-AMPK, phospho-p70S6K, phospho-mTOR, and tubulin (loading control) antibodies.
doi:10.1371/journal.pone.0070010.g006

(Invitrogen). One thousand cells were plated onto ultra-low attachment six-well plates (Corning, Corning, NY) for the sphere formation assay. The number of spheres (>100 μm in diameter) was counted on day 14 of culture. A single cell suspension derived from original spheres was obtained for the secondary sphere formation using a Neurocult chemical dissociation kit (StemCell Technologies, Vancouver, BC, Canada). Paraffin-embedded sections of spheres were subjected to hematoxylin & eosin (H&E) staining and immunostaining with anti-EpCAM (Cell Signaling Technology, Danvers, MA) and anti-AFP (Dako Cytomation, Carpinteria, CA) antibodies for the pathological analysis.

Growth Curves

The proliferation of HCC cells treated with metformin was examined using trypan blue staining after 48 and 96 hours of culture.

Detection of Apoptotic Cells

To detect apoptosis, cells were stained with an anti-CASP3 antibody (Chemicon, Temecula, CA), followed by Alexa-555-conjugated goat anti-rabbit IgG (Molecular Probes). Apoptotic cells were also evaluated by staining with Annexin V-allophycocyanin (APC) (BD Biosciences, San Jose, CA) and PI using FACSCanto (BD Biosciences).

Cell Sorting and Analysis

Single-cell suspensions were stained with an APC-conjugated anti-EpCAM antibody (Biolegend, San Diego, CA) or APC-conjugated anti-CD133/1 antibody (Miltenyi Biotec, Auburn, CA). After incubation, 1 μg/ml of PI was added to eliminate dead cells. Flow cytometric cell sorting and analysis were performed using FACSAria or FACSCanto (BD Biosciences).

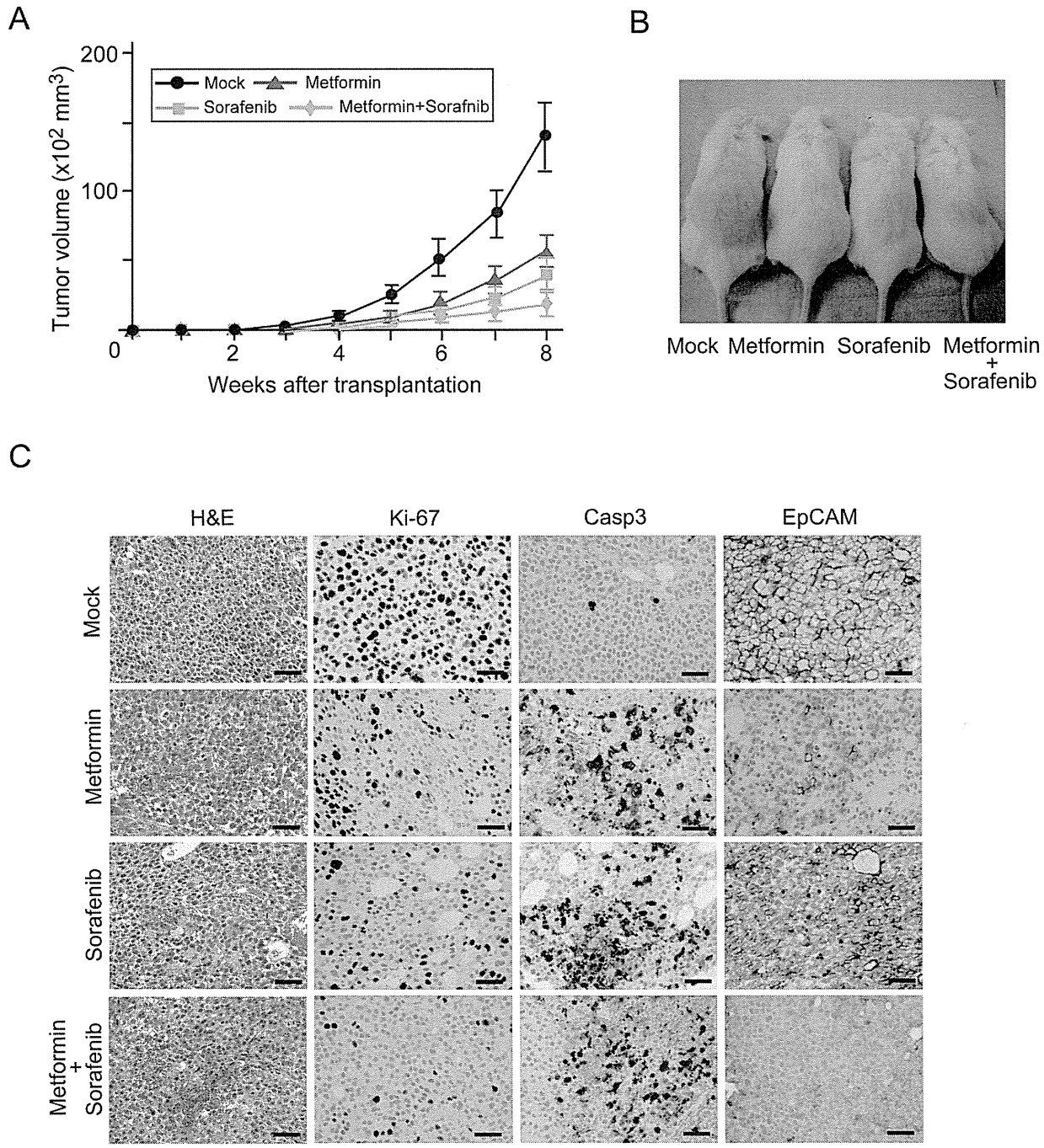

Figure 7. Inhibition of xenograft tumor growth by the administration of metformin and/or sorafenib. (A) A total of 2×10^6 Huh7 cells were transplanted into NOD/SCID mice. Tumor volume was monitored weekly after the cell transplantation. *Statistically significant ($p<0.05$). (B) Representative images of recipient mice treated with metformin and/or sorafenib 6 weeks after the transplantation. (C) Hematoxylin and eosin (H&E) staining and immunohistochemical analysis of subcutaneous tumors.
doi:10.1371/journal.pone.0070010.g007

Western Blotting

Sorted HCC cells were subjected to Western blot analysis using anti-EpCAM (Abcam, Canbridge, UK) and anti-tubulin (Oncogene Science, Cambridge, MA) antibodies. Metformin-treated cells were also subjected to Western blotting using anti-PARP (Cell Signaling Technology), anti-PCNA (Santa Cruz Biotechnologies, Santa Cruz, CA), anti-cyclin D1 (BD Biosciences), anti-p21 (Cell Signaling Technology), anti-phospho-AMPK (Cell Signaling Technology), anti-phospho-mTOR (Ser2448, Cell Signaling

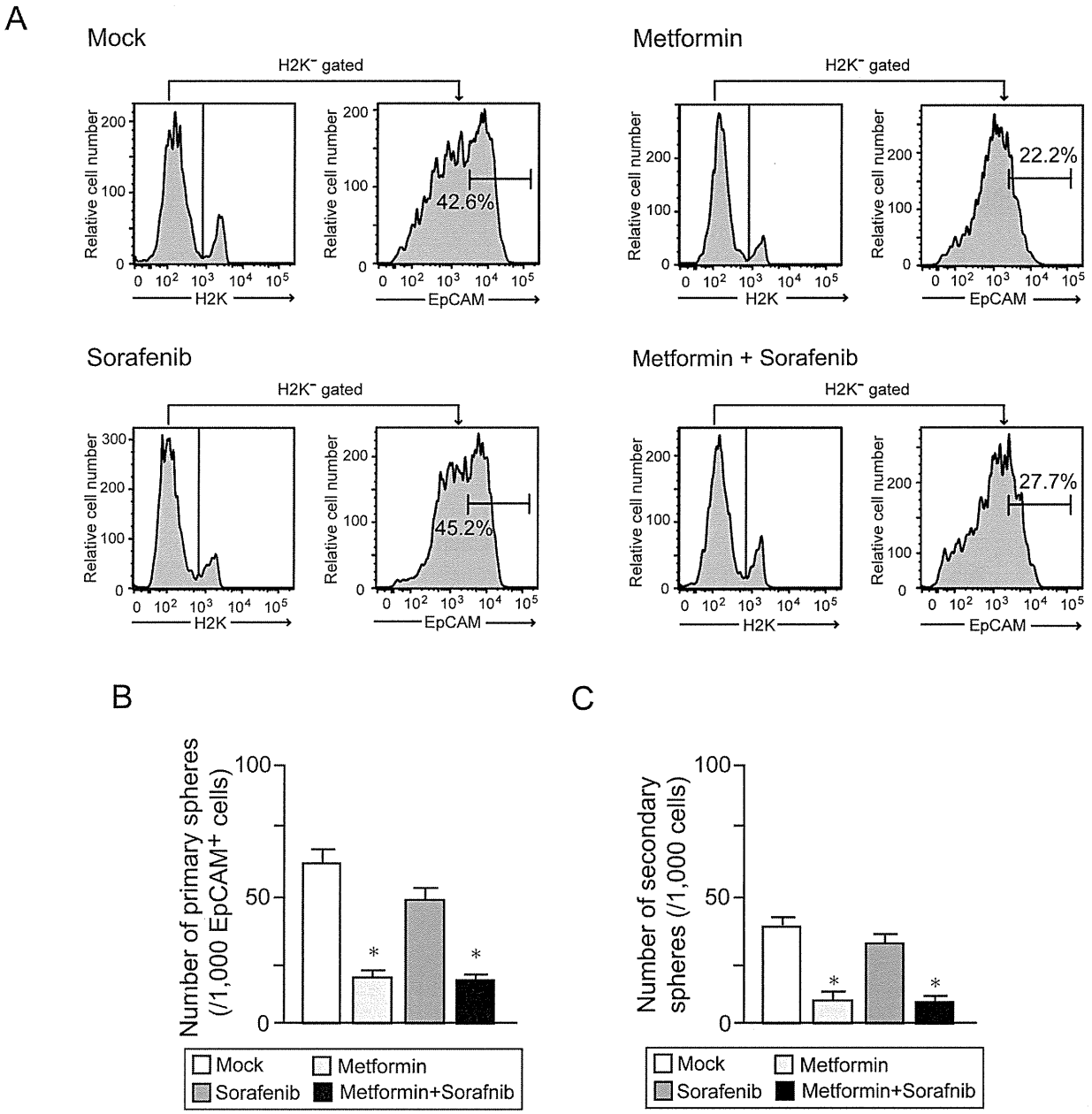

Figure 8. Re-analysis of xenograft tumors. (A) Flow cytometric analysis of subcutaneous tumors. The percentages of positive fractions for the indicated markers are shown as the mean values for three independent analyses. (B) Number of large spheres generated from 1,000 EpCAM$^+$ HCC cells treated with metformin. *Statistically significant ($p<0.05$). (C) Number of secondary spheres 14 days after replating. *Statistically significant ($p<0.05$).
doi:10.1371/journal.pone.0070010.g008

Technology), anti-phospho-p70 S6 Kinase (Thr389, Cell Signaling Technology), and anti-tubulin antibodies.

Xenograft Transplantation Using NOD/SCID Mice

In the metformin and/or sorafenib treatment model, a total of 2×10^6 Huh7 cells were transplanted into the subcutaneous space of the backs of NOD/SCID mice. Metformin (250 mg/Kg, by intraperitoneal injection) and sorafenib (10 mg/Kg, by gavage) were administered daily. Tumor formation and growth were observed weekly. To analyze subcutaneous tumors, small pieces of tumors were put in DMEM containing 5 mg/ml collagenase type II (Roche) and digested. The cell suspension was centrifuged on Ficoll (IBL, Gunma, Japan) to remove dead cells and debris. Harvested cells were subjected to flow cytometric analyses and sphere formation assays. Subcutaneous tumors were also subjected to H&E staining and immunohistochemical staining with an anti-EpCAM antibody (Cell Signaling Technology), anti-CASP3 antibody (Chemicon), and anti-Ki67 antibody (DAKO, Carpin-

teria, CA). These experiments were performed in accordance with the institutional guidelines for the use of laboratory animals.

Statistical Analysis

Data are presented as the mean ± SEM. Significant differences between 2 groups were analyzed using the Mann-Whitney U test. P values less than 0.05 were considered significant.

Author Contributions

Conceived and designed the experiments: TS TC AI OY. Performed the experiments: TS TC KY FK YZ MO SK. Analyzed the data: TM SO ES YO AT MT YT. Contributed reagents/materials/analysis tools: TS TC AI. Wrote the paper: TS TC AI.

References

1. Jordan CT, Guzman ML, Noble M (2006) Cancer stem cells. N Engl J Med 355: 1253–1261.
2. Ji J, Wang XW (2012) Clinical implications of cancer stem cell biology in hepatocellular carcinoma. Semin Oncol 39: 461–472.
3. Visvader JE, Lindeman GJ (2008) Cancer stem cells in solid tumours: accumulating evidence and unresolved questions. Nat Rev Cancer 8: 755–768.
4. Bailey CJ, Turner RC (1996) Metformin. N Engl J Med 334: 574–579.
5. Zhou G, Myers R, Li Y, Chen Y, Shen X, et al. (2001) Role of AMP-activated protein kinase in mechanism of metformin action. J Clin Invest 108: 1167–1184.
6. Evans JM, Donnelly LA, Emslie-Smith AM, Alessi DR, Morris AD (2005) Metformin and reduced risk of cancer in diabetic patients. BMJ 330: 1304–1305.
7. Bowker SL, Majumdar SR, Veugelers P, Johnson JA (2006) Increased cancer-related mortality for patients with type 2 diabetes who use sulfonylureas or insulin. Diabetes Care 29: 254–258.
8. Jalving M, Gietema JA, Lefrandt JD, de Jong S, Reyners AK, et al. (2010) Metformin: taking away the candy for cancer? Eur J Cancer 46: 2369–2380.
9. Davila JA, Morgan RO, Shaib Y, McGlynn KA, El-Serag HB (2005) Diabetes increases the risk of hepatocellular carcinoma in the United States: a population based case control study. Gut 54: 533–539.
10. Donadon V, Balbi M, Mas MD, Casarin P, Zanette G (2010) Metformin and reduced risk of hepatocellular carcinoma in diabetic patients with chronic liver disease. Liver Int 30: 750–758.
11. Chen TM, Lin CC, Huang PT, Wen CF (2011) Metformin associated with lower mortality in diabetic patients with early stage hepatocellular carcinoma after radiofrequency ablation. J Gastroenterol Hepatol 26: 858–865.
12. Yamashita T, Ji J, Budhu A, Forgues M, Yang W, et al. (2009) EpCAM-positive hepatocellular carcinoma cells are tumor-initiating cells with stem/progenitor cell features. Gastroenterology 136: 1012–1024.
13. Ma S, Chan KW, Hu L, Lee TK, Wo JY, et al. (2007) Identification and characterization of tumorigenic liver cancer stem/progenitor cells. Gastroenterology 132: 2542–2556.
14. Qu Z, Zhang Y, Liao M, Chen Y, Zhao J, et al. (2012) In vitro and in vivo antitumoral action of metformin on hepatocellular carcinoma. Hepatol Res 42: 922–933.
15. Shank JJ, Yang K, Ghannam J, Cabrera L, Johnston CJ, et al. (2012) Metformin targets ovarian cancer stem cells in vitro and in vivo. Gynecol Oncol 127: 390–397.
16. Hirsch HA, Iliopoulos D, Tsichlis PN, Struhl K (2009) Metformin selectively targets cancer stem cells, and acts together with chemotherapy to block tumor growth and prolong remission. Cancer Res 69: 7507–7511.
17. Gollob JA, Wilhelm S, Carter C, Kelley SL (2006) Role of Raf kinase in cancer: therapeutic potential of targeting the Raf/MEK/ERK signal transduction pathway. Semin Oncol 33: 392–406.
18. Yilmaz OH, Valdez R, Theisen BK, Guo W, Ferguson DO, et al. (2006) Pten dependence distinguishes haematopoietic stem cells from leukaemia-initiating cells. Nature 441: 475–482.
19. Zhou J, Wulfkuhle J, Zhang H, Gu P, Yang Y, et al. (2007) Activation of the PTEN/mTOR/STAT3 pathway in breast cancer stem-like cells is required for viability and maintenance. Proc Natl Acad Sci U S A 104: 16158–16163.
20. Dubrovska A, Kim S, Salamone RJ, Walker JR, Maira SM, et al. (2009) The role of PTEN/Akt/PI3K signaling in the maintenance and viability of prostate cancer stem-like cell populations. Proc Natl Acad Sci U S A 106: 268–273.
21. Villanueva A, Chiang DY, Newell P, Peix J, Thung S, et al. (2008) Pivotal role of mTOR signaling in hepatocellular carcinoma. Gastroenterology 135: 1972–1983.
22. Bhat M, Sonenberg N, Gores G (2013) The mTOR pathway in hepatic malignancies. Hepatology in press.
23. Zhu AX, Abrams TA, Miksad R, Blaszkowsky LS, Meyerhardt JA, et al. (2011) Phase 1/2 study of everolimus in advanced hepatocellular carcinoma. Cancer 117: 5094–5102.
24. Shirouzu Y, Ryschich E, Salnikova O, Kerkadze V, Schmidt J, et al. (2010) Rapamycin inhibits proliferation and migration of hepatoma cells in vitro. J Surg Res 159: 705–713.
25. Villanueva A, Chiang DY, Newell P, Peix J, Thung S, et al. (2008) Pivotal role of mTOR signaling in hepatocellular carcinoma. Gastroenterology 135: 1972–1983.
26. Huang S, Bjornsti MA, Houghton PJ (2003) Rapamycins: mechanism of action and cellular resistance. Cancer Biol Ther 2: 222–232.
27. Zhuang Y, Miskimins WK (2008) Cell cycle arrest in Metformin treated breast cancer cells involves activation of AMPK, downregulation of cyclin D1, and requires p27Kip1 or p21Cip1. J Mol Signal 3: 18.
28. Chen HP, Shieh JJ, Chang CC, Chen TT, Lin JT, et al. (2013) Metformin decreases hepatocellular carcinoma risk in a dose-dependent manner: population-based and in vitro studies. Gut 62: 606–615.
29. Hirsch HA, Iliopoulos D, Struhl K (2013) Metformin inhibits the inflammatory response associated with cellular transformation and cancer stem cell growth. Proc Natl Acad Sci U S A 110: 972–977.
30. Miller RA, Chu Q, Xie J, Foretz, Viollet B, et al. (2013) Biguanides suppress hepatic glucagon signalling by decreasing production of cyclic AMP. Nature 494: 256–260.
31. Cheng AL, Kang YK, Chen Z, Tsao CJ, Qin S, et al. (2009) Efficacy and safety of sorafenib in patients in the Asia-Pacific region with advanced hepatocellular carcinoma: a phase III randomised, double-blind, placebo-controlled trial. Lancet Oncol 10: 25–34.
32. Llovet JM, Ricci S, Mazzaferro V, Hilgard P, Gane E, et al. (2008) SHARP Investigators Study Group, Sorafenib in advanced hepatocellular carcinoma. N Engl J Med 359: 378–390.
33. Schmelzer E, Zhang L, Bruce A, Wauthier E, Ludlow J, et al. (2007) Human hepatic stem cells from fetal and postnatal donors. J Exp Med 204: 1973–1987.

OPEN ACCESS Freely available online

PLOS | ONE

Zoledronic Acid Produces Combinatory Anti-Tumor Effects with Cisplatin on Mesothelioma by Increasing p53 Expression Levels

Shinya Okamoto[1], Yuanyuan Jiang[2,3], Kiyoko Kawamura[2], Masato Shingyoji[4], Toshihiko Fukamachi[1], Yuji Tada[5], Yuichi Takiguchi[6], Koichiro Tatsumi[5], Hideaki Shimada[7], Kenzo Hiroshima[8], Hiroshi Kobayashi[1], Masatoshi Tagawa[2,3]*

1 Department of Biochemistry, Graduate School of Pharmaceutical Sciences, Chiba University, Chiba, Japan, **2** Division of Pathology and Cell Therapy, Chiba Cancer Center Research Institute, Chiba, Japan, **3** Department of Molecular Biology and Oncology, Graduate School of Medicine, Chiba University, Chiba, Japan, **4** Department of Thoracic Disease, Chiba Cancer Center, Chiba, Japan, **5** Department of Respirology, Graduate School of Medicine, Chiba University, Chiba, Japan, **6** Department of Medical Oncology, Graduate School of Medicine, Chiba University, Chiba, Japan, **7** Department of Surgery, School of Medicine, Toho University, Tokyo, Japan, **8** Department of Pathology, Tokyo Women's Medical University Yachiyo Medical Center, Yachiyo, Japan

Abstract

We examined anti-tumor effects of zoledronic acid (ZOL), one of the bisphosphonates agents clinically used for preventing loss of bone mass, on human mesothelioma cells bearing the wild-type *p53* gene. ZOL-treated cells showed activation of caspase-3/7, -8 and -9, and increased sub-G1 phase fractions. A combinatory use of ZOL and cisplatin (CDDP), one of the first-line anti-cancer agents for mesothelioma, synergistically or additively produced the cytotoxicity on mesothelioma cells. Moreover, the combination achieved greater anti-tumor effects on mesothelioma developed in the pleural cavity than administration of either ZOL or CDDP alone. ZOL-treated cells as well as CDDP-treated cells induced p53 phosphorylation at Ser 15, a marker of p53 activation, and up-regulated p53 protein expression levels. Down-regulation of p53 levels with siRNA however did not influence the ZOL-mediated cytotoxicity but negated the combinatory effects by ZOL and CDDP. In addition, ZOL treatments augmented cytotoxicity of adenoviruses expressing the *p53* gene on mesothelioma. These data demonstrated that ZOL-mediated augmentation of p53, which was not linked with ZOL-induced cytotoxicity, played a role in the combinatory effects with a p53 up-regulating agent, and suggests a possible clinical use of ZOL to mesothelioma with anti-cancer agents.

Citation: Okamoto S, Jiang Y, Kawamura K, Shingyoji M, Fukamachi T, et al. (2013) Zoledronic Acid Produces Combinatory Anti-Tumor Effects with Cisplatin on Mesothelioma by Increasing p53 Expression Levels. PLoS ONE 8(3): e60297. doi:10.1371/journal.pone.0060297

Editor: Dominique Heymann, Faculté de médecine de Nantes, France

Received August 15, 2012; **Accepted** February 26, 2013; **Published** March 28, 2013

Funding: This study was supported by Grants-in-Aid for Scientific Research from the Ministry of Education, Culture, Sports, Science and Technology of Japan, the Grant-in-Aid for Cancer Research from the Ministry of Health, Labor and Welfare of Japan, and a Grant-in-Aid from the Nichias Corporation. The funders had no role in study design, data collection and analysis, decision to publish, or preparation of the manuscript.

Competing Interests: The authors have the following interest. This study was partly funded by a Grant-in-Aid from the Nichias Corporation. There are no patents, products in development or marketed products to declare. This does not alter the authors' adherence to all the PLOS ONE policies on sharing data and materials, as detailed online in the guide for authors.

* E-mail: mtagawa@chiba-cc.jp

Introduction

The majority of mesothelioma development is tightly linked with occupational asbestos exposure and the patient numbers are increasing worldwide [1,2]. Approximately 70–80% of mesothelioma cells have the wild-type *p53* gene but show a homologous deletion at the INK4A/ARF locus containing the $p14^{ARF}$ and the $p16^{INK4A}$ genes, which consequently leads to decreased p53 functions despite the wild-type genotype [3–5]. Prognosis of the mesothelioma patients is dim in most of the cases [1,2,6]. Extrapleural pneumonectomy is applicable only for the patients in an early clinical stage and mesothelioma is essentially resistant to radiation. Chemotherapy is therefore the primary treatment but produced limited anti-tumor effects. A combination of cisplatin (CDDP) and pemetrexed is currently the first-line regimen but an average survival period with the agents is about 12 months [7]. The clinical outcome even with the updated combinatory chemotherapy is thus unsatisfactory and a possible second-line agent has not yet been known. A novel therapeutics is thereby required and restoration of decreased p53 functions is one of the strategies.

Bisphosphonates (BPs) are synthetic analogues of pyrophosphate and have a strong affinity for mineralized bone matrix [8]. BPs inhibit bone absorption through interfering osteoclasts' actions, and are currently used as a therapeutic agent for osteoporosis, malignancy-linked hypercalcemia and similar bone diseases. Recent reports demonstrated that BPs also achieved cytotoxicity on tumor cells through apoptosis induction and produced anti-tumor effects *in vitro* [9]. The BPs-mediated effects *in vivo* were evidenced with osseous tumors or with bone metastasis of non-osseous tumors [10]. Moreover, a number of studies also demonstrated the anti-tumor effects *in vivo* with non-osseous tumors despite BPs being readily excreted from body and accumulated in bone tissues [11,12]. The mechanism of BPs-mediated cytotoxicity is dependent on BPs structures [8,9]. The

first generation of BPs is converted into non-hydrolyzable cytotoxic ATP analogues which decrease mitochondrial membrane potentials. Both the second and the third generations inhibit farnesyl pyrophosphate synthetase and deplete isoprenoid pools, which subsequently results in decreased prenylation of small guanine-nucleotide-binding regulatory proteins (small G proteins).

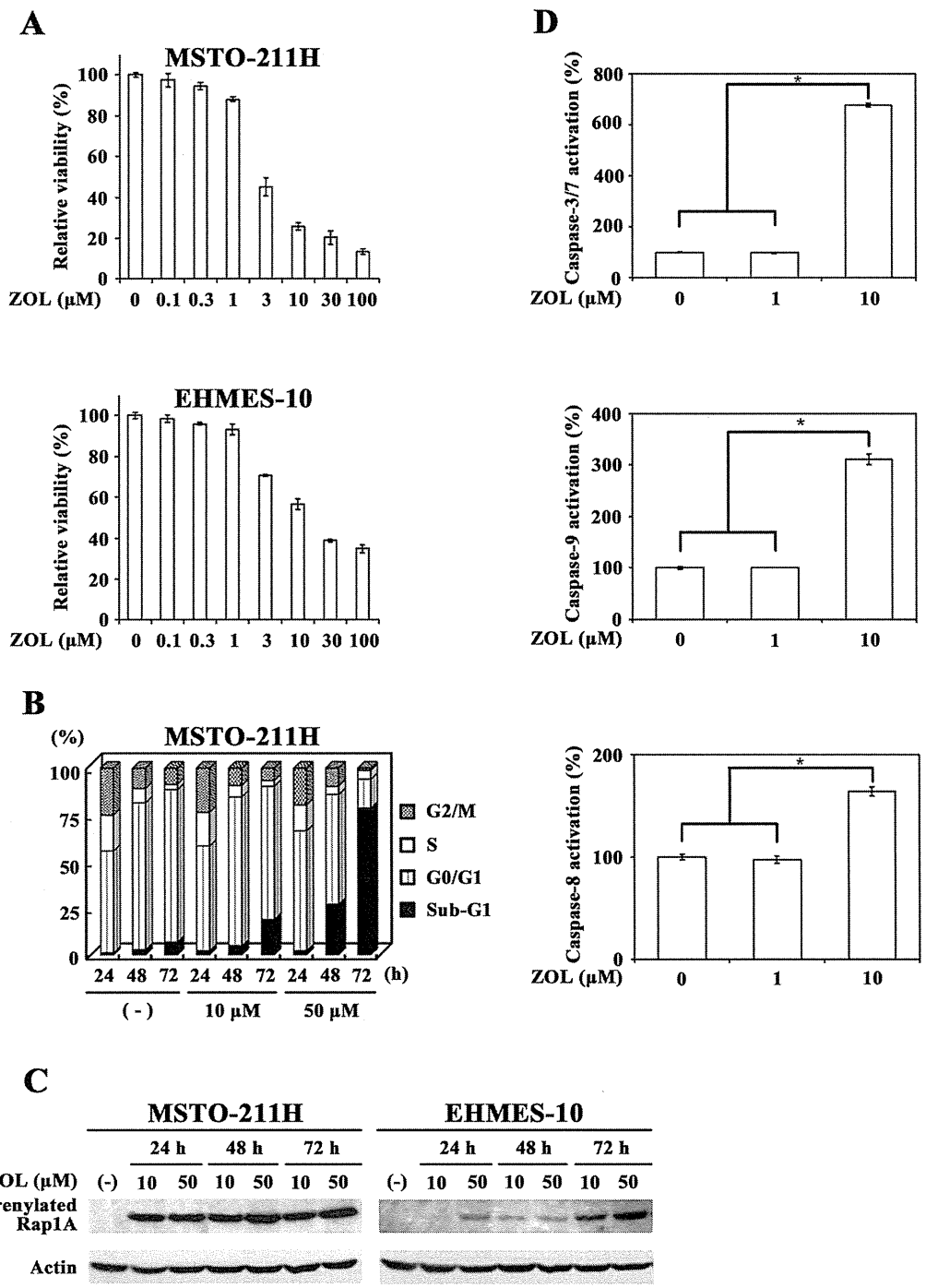

Figure 1. ZOL-induced cytotoxicity to mesothelioma. (A) Cells were treated with different concentrations of ZOL for 3 days and the cell viabilities were measured with the WST assay. Means of triplicated samples and the SD bars are shown. (B) Flow cytometrical analyses of cell cycle progression in ZOL-treated MSTO-211H cells. (C) Western blot analyses of unprenylated Rap1A expressions in cells treated with ZOL. Actin was used as a loading control. (D) Caspase activations in MSTO-211H cells that were treated with ZOL for 3 days were assayed with respective luminescence-based kits. The activities of untreated cells were expressed as 100%. Means of triplicated samples and the SE bars are shown. * $P<0.01$.
doi:10.1371/journal.pone.0060297.g001

The unprenylated form does not bind to cell membrane and the decreased membrane-bound fraction reduces functions of small G proteins since membrane binding is required for the biological activities including cell survival. It remains however uncharacterized as to the precise mechanisms of cytotoxicity induced by down-regulated functions of small G proteins.

In the present study, we examined cytotoxic activities of zoledronic acid (ZOL), one of the third generation of BPs, on human mesothelioma cells and investigated a possible combinatory use of CDDP with ZOL. We found that ZOL induced up-regulation of p53 expression and the phosphorylation, but down-regulated p53 expression had little effects on the ZOL-induced cytotoxicity. Nevertheless, the ZOL-mediated p53 activation contributed to combinatory effects with CDDP.

Materials and Methods

Cells and mice

Human mesothelioma MSTO-211H cells were purchased from American Type Culture Collection (Manassas, VA, USA) and EHMES-10 cells were kindly provided by Dr. Hamada (Ehime Univ., Ehime, Japan) [13]. Expressions of $p14^{ARF}$ and $p16^{INK4A}$ were negative and the *p53* status was wild-type in both cells. BALB/c *nu/nu* mice (6-week-old females) were purchased from Japan SLC (Hamamatsu, Japan).

Adenoviruses (Ad) preparation

Replication-incompetent type 5 Ad expressing the wild-type *p53* gene (Ad-p53) or the *β-galactosidase* gene (Ad-LacZ), in which the cytomegalovirus promoter activated transcription of the transgene, were prepared with an Adeno-X expression vector system (Takara, Shiga, Japan). The amounts of Ad were expressed as viral particles (vp).

Cell viability test

Cell viabilities were assessed with a WST reagent (Dojindo, Kumamoto, Japan) by detecting the amounts of formazan produced with absorbance at 450 nm (WST assay). The relative viability was calculated based on the absorbance without any treatments. Half maximal inhibitory concentration (IC_{50}) and combination index (CI) values at the fraction affected (Fa) which showed relative suppression levels of cell viability were calculated with CalcuSyn software (Biosoft, Cambridge, UK). Fa = 1 and Fa = 0 indicate 0% and 100% viability assayed with the WST assay, respectively, and CI<1, CI = 1 and CI>1 indicate synergistic, additive and antagonistic actions, respectively.

Cell cycle

Cells were fixed with 100% ethanol, treated with RNase A (50 μg/ml) for 15 min, and stained with propidium iodide (PI) (50 μg/ml). The fluorescence intensity was analyzed with FACSCalibur and CellQuest software (BD Biosciences, San Jose, CA, USA).

Caspase activity

Cells treated with ZOL (Novartis Pharmaceuticals, Tokyo, Japan) were tested for the activity of caspase-3/7, -8 or -9 with respective Caspase-Glo kits (Promega, Madison, WI, USA). The relative activity level was calculated based on luminescence intensity of cells without any treatments.

Western blot analysis

Cell lysate was subjected to sodium dodecyl sulfate-polyacrylamide gel electrophoresis and then transferred to a nitrocellulose membrane, which was further hybridized with antibody (Ab) against p53 (Thermo Fisher Scientific, Fremont, CA, USA), phosphorylated p53 at serine (Ser) residue 15 (Cell Signaling, Danvers, MA, USA), unprenylated Rap1A (Santa Cruz Biotechnology, Santa Cruz, CA, USA) or actin (Sigma-Aldrich, St Louis, MO, USA) as a control, followed by an appropriate second Ab. The membranes were developed with the ECL system (GE Healthcare, Buckinghamshire, UK).

RNA interference

Cells were transfected with small interfering RNA (siRNA) duplex targeting p53 or with non-coding siRNA as a control (Invitrogen, Carlsbad, CA, USA) for 24 h using Lipofectamine RNAiMAX according to the manufacturer's protocol (Invitrogen).

Animal experiments

MSTO-211H cells were injected into the pleural cavity of BALB/c *nu/nu* mice. ZOL (25 μg) or the same amount of phosphate-buffered saline (PBS) was administrated intrapleurally on day 3, and CDDP (Bristol-Myers Squibb, New York, USA) (100 μg) or the same amount of PBS was injected intraperitoneally on day 5. In this animal model, tumors became visible on day 9. The mice were sacrificed on day 24 and the tumor weights were

Table 1. Cell cycle distribution of ZOL-treated cells.

		Cell cycle distribution (% ± SE)			
ZOL (Concentration)	**Time**	**Sub-G1**	**G0/G1**	**S**	**G2/M**
(-)	24 h	1.00±0.08	54.83±0.46	19.34±0.17	25.18±0.37
(-)	48 h	2.66±0.10	78.68±0.27	7.68±0.27	10.82±0.12
(-)	72 h	6.83±0.15	82.23±0.29	2.87±0.16	8.68±0.07
10 μM	24 h	2.12±0.10	56.88±0.33	18.19±0.28	23.90±0.24
10 μM	48 h	4.75±0.13	80.28±0.13	6.13±0.19	9.38±0.14
10 μM	72 h	18.84±0.12	71.53±0.21	3.09±0.03	6.58±0.14
50 μM	24 h	2.01±0.16	64.58±0.11	13.97±0.18	19.78±0.11
50 μM	48 h	26.98±0.76	59.05±0.53	4.37±0.21	9.70±0.07
50 μM	72 h	79.14±0.32	15.65±0.13	4.73±0.06	1.22±0.11

MSTO-211H cells were treated with or without ZOL (at 10 or 50 μM) for 24–72 h. Cell cycle was analyzed with flow cytometry.
doi:10.1371/journal.pone.0060297.t001

measured. The animal experiments were approved by the animal experiment and welfare committee at Chiba University and were performed according to the guideline on animal experiments.

Results

ZOL-induced cytotoxicity and caspase activation

We examined a possible cytotoxic action of ZOL on mesothelioma cells with the WST assay and found that both mesothelioma cells, MSTO-211H and EHMES-10, were susceptible to ZOL with a dose-dependent manner (Fig. 1A). Cell cycle analyses showed that ZOL increased sub-G1 phase fractions in MSTO-211H cells (Fig. 1B, Table 1), indicating that ZOL induced cell death. We also tested ZOL-induced unprenylation of Rap 1A, one of small G proteins, and confirmed that ZOL inhibited the prenylation in both cells (Fig. 1C). We investigated a possible activation of caspase-3/7, -9 and -8 by testing the cleaving activity of a specific substrate (Fig. 1D). ZOL treatments at 1 μM did not induce activation of respective caspases but those at 10 μM activated the caspases in MSTO-211H cells. These data collectively indicated that ZOL treatments activated cell death processes through the caspase cleavages in mesothelioma cells.

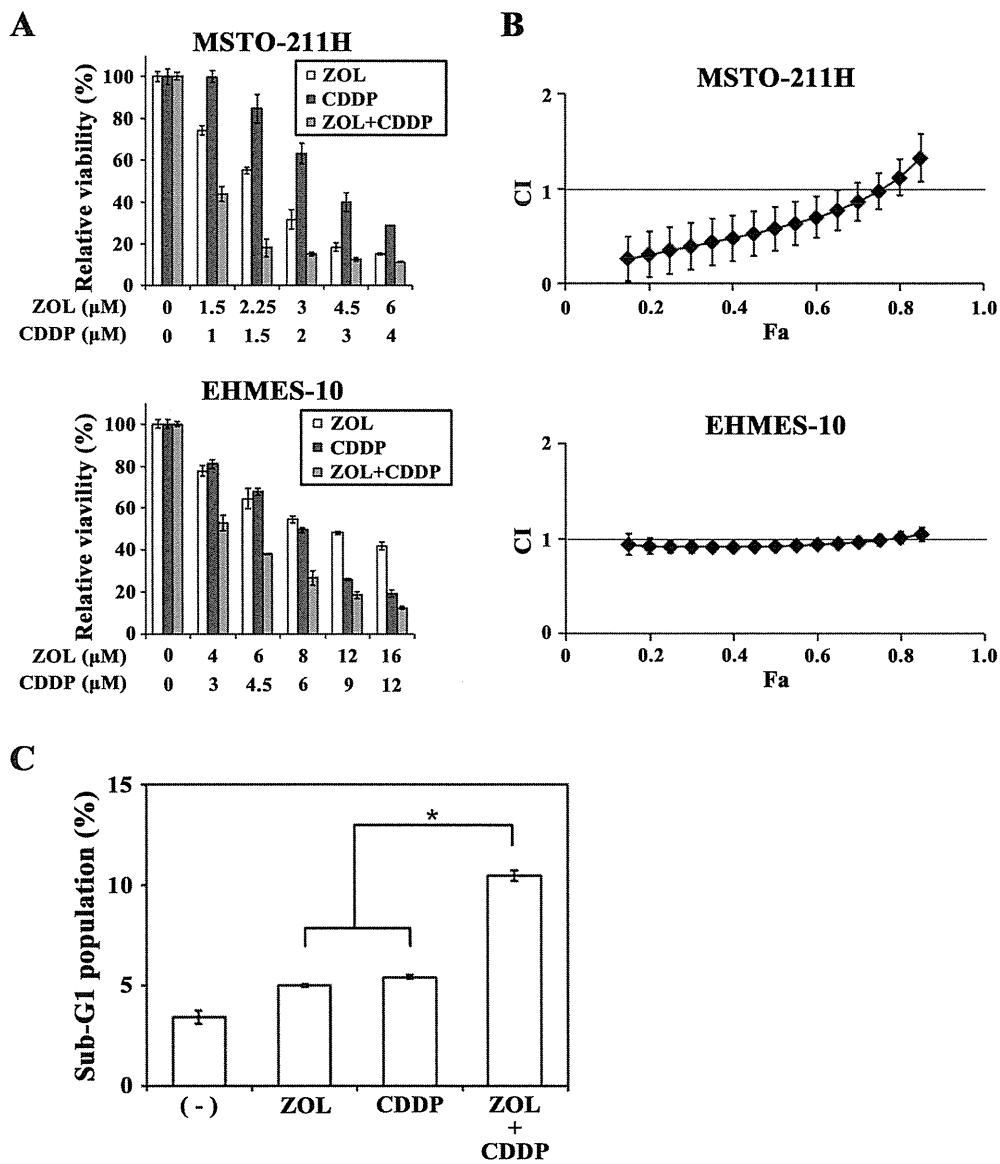

Figure 2. Combinatory effects of ZOL and CDDP. (A) Cells were treated with different doses of ZOL and CDDP at a constant concentration ratio (ZOL:CDDP = 3:2 at each concentration in MSTO-211H and 4:3 in EHMES-10 cells) for 3 days and the cell viabilities were measured with the WST assay. Means of triplicated samples and the SD bars are shown. (B) CI values based on the cell viabilities as shown in (A) were calculated at different Fa points with CalcuSyn software. The SE bars are also indicated. (C) Sub-G1 phase populations of PI-stained MSTO-211H cells that were treated with ZOL (15 μM) and/or CDDP (4 μM) for 24 h were calculated with flow cytometry. Means of triplicated samples and the SE bars are shown. * $P<0.01$.
doi:10.1371/journal.pone.0060297.g002

Combinatory cytotoxic effects of ZOL and CDDP

We investigated combinatory effects of ZOL and CDDP in MSTO-211H and EHMES-10 cells. We calculated respective IC_{50} values of each agent to know an optimal test rang and then examined cytotoxicity at various doses of both agents with a constant concentration ratio according to the CalcuSyn software instruction. Combination of ZOL and CDDP achieved cytotoxicity greater than each agent (Fig. 2A) and statistical analyses showed that CI values at Fa points below 0.8 in MSTO-211H cells were less than 1 and those between 0.15 and 0.8 Fa points in EHMES-10 cells were close to but under 1 (Fig. 2B). These CI values demonstrated that both ZOL and CDDP achieved cytotoxicity synergistically in MSTO-211H cells, and additively, or possibly slightly synergistically, in EHMES-10 cells. Cell cycle analyses indicated that sub-G1 phase populations in ZOL- plus CDDP-treated MSTO-211H cells were greater than those in ZOL- or CDDP- treated cells (Fig. 2C), suggesting that the enhanced cytotoxic activities by the combination of ZOL and CDDP were attributable to increased apoptotic cell death.

Combinatory effects of ZOL and CDDP *in vivo*

We investigated anti-tumor effects of ZOL in combination with CDDP in an orthotopic animal model (Fig. 3). Nude mice injected with MSTO-211H cells in the pleural cavity received ZOL intrapleurally and/or CDDP intraperitoneally. All the tumors were found in the pleural cavity without any detectable extrapleural metastatic foci. ZOL or CDDP administration inhibited the tumor growth compared with PBS-injected group. A combinatory administration of ZOL and CDDP further decreased tumor weights, demonstrating that the combination produced greater therapeutic effects than the case treated with a single agent. We did not notice body weight loss in the combinatory group, indicating that the combination was not toxic to the tested animals.

ZOL induced p53 activation

We examined whether p53 activation was involved in the ZOL-mediated cytotoxicity since the p53 pathways play a key role in apoptosis induction. Firstly, we tested possible p53 activation in wild-type *p53* mesothelioma with CDDP (Fig. 4A). CDDP-treated MSTO-211H and EHMES-10 cells induced phosphorylation of p53 at the Ser 15 residue, a hallmark of p53 activation, and up-regulated p53 protein levels. We then examined influence of ZOL on p53 expressions and found that ZOL treatments phosphorylated p53 at Ser 15 and augmented p53 protein levels in both cells (Fig. 4B). These data showed that ZOL induced p53 activation and subsequently raised a possibility that the ZOL-mediated cytotoxicity was caused by p53 activation. We also investigated the combinatory effects of CDDP and ZOL on the p53 phosphorylation at Ser 15 (Fig. 4C). The phosphorylation level in cells treated with both agents was greater than that in cells treated with either CDDP or ZOL, suggesting that both agents cooperatively activated the p53 pathways.

Down-regulated p53 action on cytotoxicity and on combination effect

We further investigated a possible involvement of p53 activation in the ZOL-mediated cytotoxicity by down-regulating p53 expression with siRNA. The p53-siRNA treatment markedly decreased p53 expression and the phosphorylation level (Fig. 4D). The down-regulated p53 however minimally affected the ZOL-induced cytotoxicity in MSTO-211H cells, at least in lower concentrations, and rather slightly enhanced the cytotoxicity in

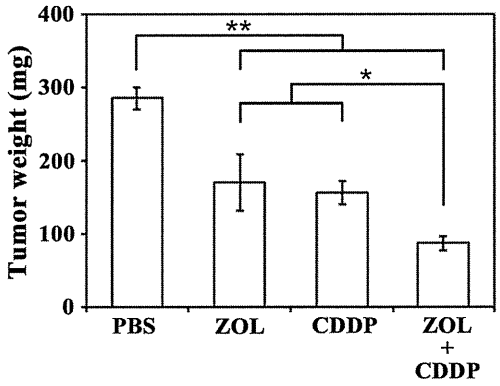

Figure 3. Combinatory effects with ZOL and CDDP in an orthotopic animal model. MSTO-211H cells (1×10^6) were inoculated into the pleural cavity of BALB/c *nu/nu* mice (n = 6) (day 1), and then ZOL (25 μg, day 3) was administrated into the pleural cavity and/or CDDP (100 μg, day 5) into the peritoneal cavity (CDDP). PBS was used as a control. Tumor weights were measured on day 24. The SE bars are also shown. * $P<0.05$, ** $P<0.01$.
doi:10.1371/journal.pone.0060297.g003

EHMES-10 cells (Fig. 4E). Control siRNA treatments unexpectedly increased the cytotoxicity in MSTO-211H cells at high ZOL concentrations. These data suggested that the ZOL-mediated cytotoxicity was independent of p53 activation. We also analyzed cell cycle changes in ZOL-treated MSTO-211H cells after they were transfected with p53-siRNA (Fig. 4F, Table 2). Cell cycle distributions showed that p53-siRNA treatments marginally influenced the ZOL-mediated increase of sub-G1 phase populations. The decreased level of sub-G1 phase fractions due to the p53-siRNA treatment was disproportionately lower than that of the p53 protein expression after transfection with siRNA. In contract, the p53-siRNA treatment increased S and G2/M phase and decreased G0/G1 phase fractions, showing that down-regulated p53 promoted cell cycle progression. These data demonstrated that decreased p53 levels influenced the cell cycle but little affected the ZOL-mediated cytotoxicity, and confirmed that the ZOL-induced p53 activation was irrelevant to the ZOL-mediated cytotoxicity. Control-siRNA treated cells increased sub-G1 phase fractions, which accorded with the WST results. It could be due to non-specific cytotoxicity of control siRNA in MSTO-211H cells but the mechanism underling is currently unknown.

We also examined whether the combinatory effects of ZOL and CDDP were modulated by p53 expression levels (Fig. 4G and H). The p53-siRNA treatments nullified the synergistic or the additive effects detected in MSTO-211H and EHMES-10 cells. The CI values of the combination under the p53-siRNA treatments were more than 1, which indicated rather antagonistic actions. Activation of p53 was thus involved in the combinatory effects of ZOL and CDDP although it was not related with the ZOL-mediated cytotoxicity.

Combinatory effects of ZOL and Ad-p53

We examined whether up-regulated p53 levels by ZOL increased p53-mediated cytotoxicity. Transduction of MSTO-211H cells with Ad-p53 but not Ad-LacZ increased p53 expressions and induced the phosphorylation at Ser 15 (Fig. 5A). Moreover, Ad-p53 but not Ad-LacZ decreased the cell viability with a dose-dependent manner (Fig. 5B), demonstrating that induction of p53 produced cytotoxic effects in MSTO-211H cells. We then examined combinatory effects of Ad-p53 and ZOL at a

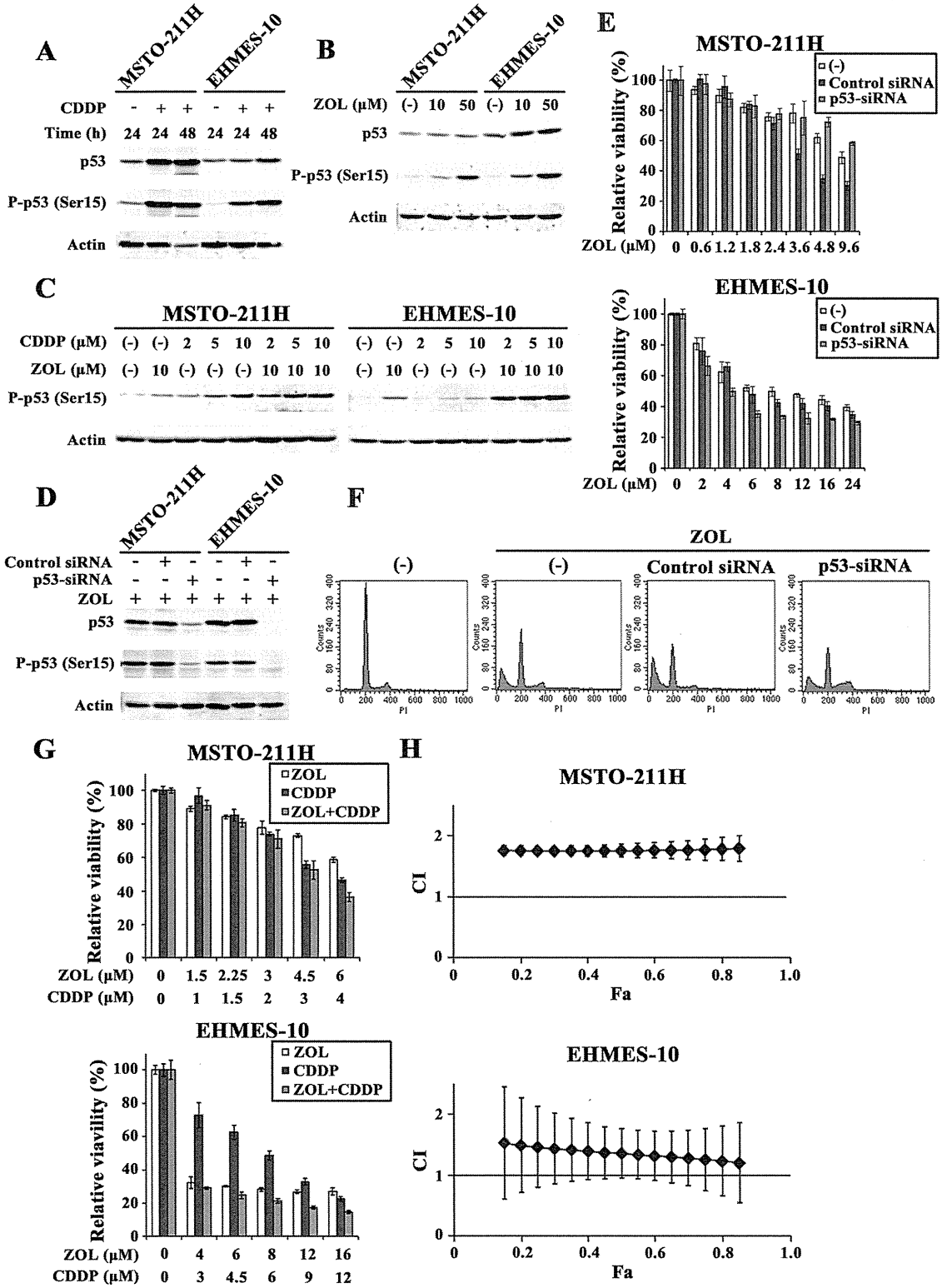

Figure 4. ZOL-induced up-regulation of p53 and knockdown of the p53 expressions with siRNA. (A, B) CDDP-treated (20 μM) and ZOL-treated (48 h) cells were subjected to Western blot analysis and probed with antibodies as indicated. Actin was used as a loading control. (C) Cells were treated with CDDP and/or ZOL for 48 h at the indicated concentrations and the expression levels of phosphorylated p53 were examined. (D) Cells were transfected with p53-targeted siRNA (p53-siRNA) or non-targeted control siRNA (Control) for 24 h and then treated with ZOL (50 μM) for

48 h. The lysate was subjected to Western blot analysis. (E) Cells were transfected with siRNA as indicted and were treated with ZOL for 3 days. The cell viabilities were measured with the WST assay and means of triplicated samples with the SD bars are shown. (F) Flow cytometrical analyses of MSTO-211H cells that were transfected with respective siRNA for 24 h and then treated with ZOL (50 μM) for 48 h. (G, H) Cells transfected with p53-siRNA were treated with different doses of ZOL and CDDP as indicated for 3 days and the CI values based on the cell viabilities were calculated at different Fa points with CalcuSyn software.
doi:10.1371/journal.pone.0060297.g004

constant ratio between the agents (Fig. 5C). The combination produced additive, or possibly slightly synergistic, effects at above 0.15 Fa points. (Fig. 5D) and suggested that up-regulation of p53 by ZOL enhanced Ad-p53-mediated cytotoxicity by further activating the p53 pathways.

Discussion

In this study we demonstrated that ZOL alone and the combination with CDDP produced anti-tumor effects on mesothelioma. ZOL up-regulated p53 expression but the ZOL-mediated cytotoxicity was scarcely dependent on the p53 induction, suggesting that the cytotoxicity was due to inhibition of small G proteins' functions. Down-regulated p53 levels on the other hand negated the synergistic actions by ZOL and CDDP, indicating that the ZOL-induced p53 activation contributed to the combinatory anti-tumor effects produced with CDDP.

The majority of mesothelioma cells has defect of $p14^{ARF}$, which results in an increased level of Mdm2 that induces p53 degradation [14,15]. Augmentation of p53 is therefore a possible therapeutic strategy for mesothelioma by restoring p53 functions [16]. The present study indicated that ZOL phosphorylated p53 and up-regulated the expression levels, suggesting a crucial role of p53 induction in the ZOL-mediated cytotoxicity. ZOL in fact activated caspases and increased sub-G1 phase populations. The knockdown experiments with p53-siRNA however demonstrated that p53 activation itself did not contribute to the ZOL-mediated cytotoxic actions. A possible involvement of the p53 pathways in ZOL-mediated cytotoxicity may need further investigations but the present data evidenced that the up-regulated p53 level in ZOL-treated cells was irrelevant to the cytotoxicity as reported previously [17,18]. The ZOL-induced cytotoxicity can be therefore attributable to inhibited prenylation of small G proteins [8–10].

ZOL-induced activation of p53 nevertheless contributed to the cytotoxicity by other agents of which the functions were linked with p53 levels. CDDP is one of such agents and augmented p53 levels in target tumors facilitate CDDP-induced cell death [19,20]. In fact our previous study showed that Ad-p53-transduced MSTO-211H cells produced synergistic cytotoxicity with CDDP, and that the CI values were below 1 between 0.2 and 0.8 Fa points [21]. The present study demonstrated that combination of ZOL and CDDP produced synergistic or additive anti-tumor effects on mesothelioma with the wild-type *p53* gene. The combination increased sub-G1 phase populations and decreased tumor volumes in an orthotopic animal model, but down-regulation of p53 with the siRNA completely nullified the combinatory effects. These data suggested that ZOL-induced p53 up-regulation favored CDDP-mediated cytotoxicity through further augmenting the p53 pathways. Benassi *et al* recently reported similar results with paired cells, *p53*-mutated and the isogeneic *p53*-wild-type parent cells from osteosarcoma, that combinatory effects of ZOL and CDDP were p53-dependent [20]. The present study furthermore analyzed the interactions between the two agents and demonstrated synergistic or additive actions in the combination as well as the *in vivo* efficacy. The interactions became antagonistic under the p53-siRNA treatment, which suggested that loss of ZOL-induced p53 up-regulation was rather inhibitory to CDDP-mediated cytotoxicity. These data consequently suggest that the ZOL-mediated up-regulated p53 pathways contributed to combinatory effects with CDDP. ZOL-mediated inhibitory actions on small G proteins' prenylation were probably not influenced by cellular p53 levels because down-regulation of p53 did not affect the ZOL-mediated cytotoxicity. The inhibited prenylation itself may produce possible combinatory effects with CDDP but the p53-siRNA treatment which produced antagonistic effects suggested that mechanistic association between unprenylated small G proteins and CDDP was unlikely.

Transduction levels of Ad-p53 determined p53-dependent cytotoxicity, and a combinatory use of ZOL and Ad-p53 produced additive, and possibly slightly synergistic, cytotoxic effects. A possible role of Ad-p53 in the combinatory effects through inducing further unpreylation of small G proteins was probably minimal since ZOL-mediated cytotoxicity was independent of p53 levels. Nevertheless, ZOL augmented endogenous p53 levels and the up-regulation appeared to sensitized tumor cells to be susceptible to a p53 up-regulating agent. ZOL can induce unprenylation of non-small G proteins but it remains uncharacterized whether such unprenylated non-small G proteins can produce cytotoxicity in ZOL-treated cells. Synergism between CDDP and ZOL was greater than that between Ad-p53 and ZOL probably because CDDP-mediated p53 up-regulation and over-expression of p53 with Ad-p53 are not equal from the standpoint of signal transduction systems. For example, CDDP-treated cells can activate non-p53-mediated pathways and Ad-mediated transduction activates type I interferons-mediated pathways.

The present data suggested a possible clinical application of ZOL for mesothelioma in combination with CDDP or Ad-p53. In fact, Ad-p53 has been used in clinical trials [22], and ZOL and CDDP are commonly used for cancer patients [8,23]. We demonstrated combinatory anti-tumor effects of ZOL and CDDP on non-osseous tumors as reported on osseous tumors [20,24]. Therapeutic activities of ZOL on tumors nevertheless seem to be less significant in non-osseous tissues than those in osseous tissues [9,10] because ZOL is readily excreted from kidney and cannot be maintained at a high concentration except in bone tissues [10,11]. Recent studies however showed that ZOL in combination with imatinib and doxorubicin produced greater cytotoxicity than monotherapy even against non-osseous tumors, Bcr-Abl-positive

Table 2. Cell cycle distribution of p53-siRNA-treated cells.

		Cell cycle distribution (% ± SE)			
siRNA for	**ZOL**	**Sub-G1**	**G0/G1**	**S**	**G2/M**
(−)	(−)	2.35±0.07	81.69±0.36	6.88±0.29	8.79±0.33
(−)	(+)	34.53±0.23	50.39±0.13	6.12±0.11	8.32±0.29
Control	(+)	52.34±0.60	38.23±0.32	3.79±0.08	5.10±0.27
p53	(+)	28.36±0.12	38.59±0.16	16.69±0.17	15.53±0.17

MSTO-211H cells were transfected with or without siRNA for 24 h, and then treated with or without 50 μM ZOL for further 48 h. Cell cycle was analyzed with flow cytometry.
doi:10.1371/journal.pone.0060297.t002

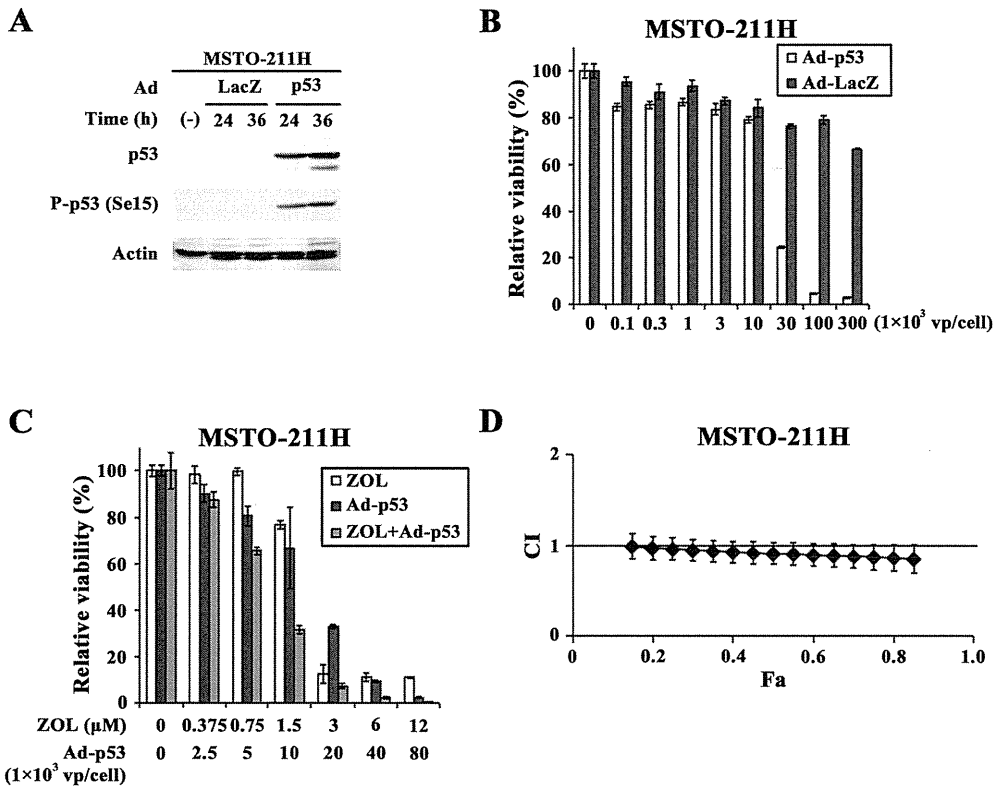

Figure 5. Combinatory effects with ZOL and Ad-p53. (A) Cells were infected with Ad-p53 or Ad-LacZ (1×10^3 vp/cell) as a control and were subjected to Western blot analysis. Actin was used as a loading control. (B) Cells were infected with Ad-p53 or Ad-LacZ and the cell viabilities were measured with the WST assay. Means of triplicated samples and the SD bars are shown. (C, D) Cells were infected with Ad-p53 and/or treated with ZOL as indicated and cultured for 3 days. The cell viabilities were measured with the WST assay and CI values based on the cell viabilities were calculated at different Fa points with CalcuSyn software.
doi:10.1371/journal.pone.0060297.g005

leukemina [25] and breast cancer [26], respectively. These data indicated that ZOL, even through a systemic administration route, produced anti-tumor effects together with other cytotoxic agents. Moreover, mesothelioma can be one of the suitable targets of ZOL in clinical settings because the intrapleural administration is speculated to keep a relative high concentration of ZOL at tumor sites compared with an intravenous injection, although this remains to be proven. The present study suggests that ZOL administered intrapleurally and CDDP injected systemically may produce a therapeutic benefit to mesothelioma patients. Our preliminary study showed that intrapleural administration of 40 μg ZOL at a concentration of 0.4 mg/ml in mice, which was equivalent to 7.8–9.8 mg in human [27] and was 10 times higher drug concentration than the current clinical dose (4 mg in total and 0.04 mg/ml at the concentration), did not cause any body weight changes or other adverse reactions such as inflammatory reactions (data not shown), showing a feasible intrapleural injection of ZOL with safe.

We also showed that Ad-p53 suppressed the viability of mesothelioma and produced combinatory anti-tumor effects with ZOL. Intrapleural injections of Ad-p53 were in fact conducted safely in patients with pleural effusions [28]. Previous studies demonstrated that Ad-p53 activated the p53 pathways and achieved combinatory anti-tumor effects with an anti-cancer agent including CDDP [21,29,30]. The mechanism of ZOL-mediated p53 induction remains unclear but the p53-inducible p21 is a downstream target of Ras and RhoA, the major molecules of small G proteins [31]. Inhibited protein prenylation can cause downstream activation of p53, and ZOL thereby is a candidate to analyze a possible cross-talk between small G proteins and the p53 pathways. Previous studies also showed that combinatory cytotoxicity of ZOL and an anti-cancer agent was linked with ZOL-mediated inhibition of P-glycoprotein functions [24] and that a combinatory use of doxorubicin and ZOL inhibited angiogenesis [26]. These studies indicated possible p53-independent cytotoxicity of ZOL that could synergize with other agents through multiple mechanisms.

In conclusion, we demonstrated that ZOL produced cytotoxic activities on mesothelioma and a combinatory use with CDDP or Ad-p53 produced better therapeutic effects than monotherapy with a single agent. ZOL-mediated p53 up-regulation was not involved in the ZOL-induced cytotoxicity in EHMES-10 cells, and in MSTO-211H cells at least at low concentrations at which synergistic effects were observed with CDDP, but contributed to combinatory anti-tumor effects of CDDP or Ad-p53. Based on the current study we presume that an intrapleural injection of ZOL, which is technically feasible, in combination with CDDP, the first-line agent for mesothelioma, is a potential therapeutics for mesothelioma.

Acknowledgments

We appreciate Ms. Yoshie Chiba for helpful discussion.

Author Contributions

Conceived and designed the experiments: TF Y. Takiguchi KT HK MT. Performed the experiments: SO YJ KK MS Y. Tada. Contributed reagents/materials/analysis tools: HS KH. Wrote the paper: SO MT.

References

1. Tada Y, Takiguchi Y, Hiroshima K, Hiroshima K, Shimada H, et al. (2008) Gene therapy for malignant pleural mesothelioma: Present and Future. Oncol Res 17: 239–246.
2. Robinson BWS, Lake RA (2005) Advances in malignant mesothelioma. N Engl J Med 353: 1591–1603.
3. Altomare DA, Menges CW, Xu J, Pei J, Zhang L, et al (2011) Losses of both products of the *Cdkn2a/Arf* locus contribute to asbestos-induced mesothelioma development and cooperate to accelerate tumorigenesis. PLoS ONE 6. e18828. doi:10.1371/journal.pone.0018828.
4. Prins JB, Williamson KA, Kamp MMK, Van Hezink EJ, Van Der Kwast TH, et al (1998) The gene for the cyclin-dependent-kinase-4 inhibitor, *CDKN2A*, is preferentially deleted in malignant mesothelioma. Int J Cancer 75: 649–653.
5. Altomare DA, Menges CW, Pei J, Zhang L, Skele-Stump KL, et al. (2009) Activated TNF-α/NF-κB signaling via down-regulation of Fas-associated factor 1 in asbestos-induced mesothelioma from *Arf* knockout mice. Proc Natl Acad Sci USA 106: 3420–3425.
6. Robinson BWS, Musk AW, Lake RA (2005) Malignant mesothelioma. Lancet 366: 397–408.
7. Vogelzang NJ, Rusthoven JJ, Symanowski J, Denham C, Kaukel E, et al. (2003) Phase III study of pemetrexed in combination with cisplatin versus cisplatin alone in patients with malignant pleural mesothelioma. J Clin Oncol 21: 2636–2644.
8. Yuasa T, Kimura S, Ashihara E, Habuchi T, Maekawa T (2007) Zoledronic acid -a multiplicity of anti-cancer action. Curr Med Chem 14: 2126–2135.
9. Green JR (2003) Antitumor effects of bisphosphonates. Cancer 97 (Suppl 3):840–847.
10. Green JR (2004) Bisphosphonates: preclinical review. Oncologist 9 (Suppl 4): 3–13.
11. Skerjanec A, Berenson J, Hsu C, Major P, Miller WH Jr, et al. (2003) The pharmacokinetics and pharmacodynamics of zoledronic acid in cancer patients with varying degrees of renal function. J Clin Pharmacol 43: 154–162.
12. Clézardin P (2011) Bisphosphonates' antitumor activity: an unravelled side of a multifaceted drug class. Bone 48: 71–79.
13. Nakataki E, Yano S, Matsumori Y, Goto H, Kakiuchi S, et al. (2006) Novel orthotopic implantation model of human malignant pleural mesothelioma (EHMES-10 cells) highly expressing vascular endothelial growth factor and its receptor. Cancer Sci 97: 183–191.
14. Yang CT, You L, Yeh CC, Chang JWC, Zhang F, et al. (2000) Adenovirus-mediated $p14^{ARF}$ gene transfer in human mesothelioma cells. Natl Cancer Inst 92: 636–641.
15. Kim WY, Sharpless NE (2006) The regulation of *INK4/ARF* in cancer and aging. Cell 127: 265–275.
16. Hoskins-Donaldson S, Belyanskaya LL, Simões-Wüst AP, Sigrist B, Kurtz S, et al. (2006). p53-induced apoptosis occurs in the absence of $p14^{ARF}$ in malignant pleural mesothelioma. Neoplasia 8: 551–559.
17. Kuroda J, Kimura S, Segawa H, Sato K, Matsumoto S, et al. (2004) p53-independent anti-tumor effects of the nitrogen-containing bisphosphonate zoledronic acid. Cancer Sci 95: 186–192.
18. Ory B, Blanchard F, Battaglia S, Gouin F, Rédini F, et al. (2007) Zoledronic acid activates the DNA S-phase checkpoint and induces osteosarcoma cell death characterized by apoptosis-inducing factor and endonuclease-G translocation independently of p53 and retinoblastoma status. Mol Pharmacol 71: 333–343.
19. Siddik ZH (2003) Cisplatin: mode of cytotoxic action and molecular basis of resistance. Oncogene 22: 7265–7279.
20. Benassi MS, Chiechi A, Ponticelli F, Pazzaglia L, Gamberi G, et al. (2007) Growth inhibition and sensitization to cisplatin by zoledronic acid in osteosarcoma cells. Cancer Lett 250: 194–205.
21. Li Q, Kawamura K, Okamoto S, Yamanaka M, Yang S, et al (2012) Upregulated p53 expression activates apoptotic pathways in wild-type *p53*-bearing mesothelioma and enhances cytotoxicity of cisplatin and pemetrexed. Cancer Gene Ther 19: 218–228.
22. Senzer N, Nemunaitis J, Nemunaitis M, Lamont J, Gore M, et al. (2007) *p53* therapy in a patient with Li-Fraumeni syndrome. Mol Cancer Ther 6: 1478–1482.
23. Rossi A, Di Maio M, Chiodini P, Rudd RM, Okamoto H, et al. (2012) Carboplatin- or cisplatin-based chemotherapy in first-line treatment of small-cell lung cancer: the COCIS meta-analysis of individual patient data. J Clin Oncol 30: 1692–1698.
24. Horie H, Murata H, Kimura S, Takeshita H, Sakabe T, et al. (2007) Combined effects of a third-generation bisphosphonate, zoledronic acid with other anticancer agents against murine osteosarcoma. Brit J Cancer 96: 255–261.
25. Kuroda J, Kimura S, Segawa H, Kobayashi Y, Yoshikawa T, et al. (2003) The third-generation bisphosphonate zoledronate synergistically augments the anti-Ph^+ leukemia activity of imatinib mesylate. Blood 102: 2229–2235.
26. Ottewell PD, Mönkkönen H, Jones M, Lefley DV, Coleman RE, et al. (2008) Antitumor effects of doxorubicin followed by zoledronic acid in a mouse model of breast cancer. J Natl Cancer Inst 100: 1167–1178.
27. Reagan-Shaw S, Nihal M, Ahmad N (2008) Dose translation from animal to human studies revisited. FASEB J 22: 659–661.
28. Liu DH, Liu WC, Fan Li, Sheng R, Xue Y, et al. (2006) Clinical effect of p53 gene Gendicine in treatment. Chin J Cancer Prev Treat 13: 1108–1109.
29. Horio Y, Hasegawa Y, Sekido Y, Takahashi M, Roth JA, et al. (2000) Synergistic effects of adenovirus expressing wild-type p53 on chemosensitivity of non-small cell lung cancer cells. Cancer Gene Ther 7: 537–544.
30. Weinrib L, Li JH, Donovan J, Huang D, Liu FF (2001) Cisplatin chemotherapy plus adenoviral *p53* gene therapy in EBV-positive and -negative nasopharyngeal carcinoma. Cancer Gene Ther 8: 352–360.
31. Bar-Sagi D, Hall A (2000) Ras and Rho GTPases: a family reunion. Cell 103: 227–238.

Interferon-β Produces Synergistic Combinatory Anti-Tumor Effects with Cisplatin or Pemetrexed on Mesothelioma Cells

Quanhai Li[1,2], Kiyoko Kawamura[1], Shan Yang[1,2], Shinya Okamoto[3], Hiroshi Kobayashi[3], Yuji Tada[4], Ikuo Sekine[5], Yuichi Takiguchi[5], Masato Shingyouji[6], Koichiro Tatsumi[4], Hideaki Shimada[7], Kenzo Hiroshima[8], Masatoshi Tagawa[1,2*]

1 Division of Pathology and Cell Therapy, Chiba Cancer Center Research Institute, Chiba, Japan, **2** Department of Molecular Biology and Oncology, Graduate School of Medicine, Chiba University, Chiba, Japan, **3** Department of Biochemistry, Graduate School of Pharmaceutical Science, Chiba University, Chiba, Japan, **4** Department of Respirology, Graduate School of Medicine, Chiba University, Chiba, Japan, **5** Department of Medical Oncology, Graduate School of Medicine, Chiba University, Chiba, Japan, **6** Division of Thoracic Diseases, Chiba Cancer Center, Chiba, Japan, **7** Department of Surgery, School of Medicine, Toho University, Tokyo, Japan, **8** Department of Pathology, Tokyo Women's Medical University Yachiyo Medical Center, Yachiyo, Japan

Abstract

Interferons (IFNs) have been tested for the therapeutic effects in various types of malignancy, but mechanisms of the anti-tumors effects and the differential biological activities among IFN members are dependent on respective cell types. In this study, we examined growth inhibitory activities of type I and III IFNs on 5 kinds of human mesothelioma cells bearing wild-type *p53* gene, and showed that type I IFNs but not type III IFNs decreased the cell viabilities. Moreover, growth inhibitory activities and up-regulated expression levels of the major histocompatibility complexes class I antigens were greater with IFN-β than with IFN-α treatments. Cell cycle analyses demonstrated that type I IFNs increased S- and G2/M-phase populations, and subsequently sub-G1-phase fractions. The cell cycle changes were also greater with IFN-β than IFN-α treatments, and these data collectively showed that IFN-β had stronger biological activities than IFN-α in mesothelioma. Type I IFNs-treated cells increased p53 expression and the phosphorylation levels, and activated apoptotic pathways. A combinatory use of IFN-β and cisplatin or pemetrexed, both of which are the current first-line chemotherapeutic agents for mesothelioma, produced synergistic anti-tumor effects, which were also evidenced by increased sub-G1-phase fractions. These data demonstrated firstly to our knowledge that IFN-β produced synergistic anti-tumor effects with cisplatin or pemetrexed on mesothelioma through up-regulated p53 expression.

Citation: Li Q, Kawamura K, Yang S, Okamoto S, Kobayashi H, et al. (2013) Interferon-β Produces Synergistic Combinatory Anti-Tumor Effects with Cisplatin or Pemetrexed on Mesothelioma Cells. PLoS ONE 8(8): e72709. doi:10.1371/journal.pone.0072709

Editor: Fabrizio Mattei, Istituto Superiore di Sanità, Italy

Received February 15, 2013; **Accepted** July 15, 2013; **Published** August 16, 2013

Funding: Grants-in-Aid for Scientific Research from the Ministry of Education, Culture, Sports, Science and Technology of Japan, the Grant-in-Aid for Research on seeds for Publicly Essential Drugs and Medical Devices from the Ministry of Health, Labor and Welfare of Japan, and a Grant-in-aid from the Nichias Corporation. The funders had no role in study design, data collection and analysis, decision to publish, or preparation of the manuscript.

Competing interests: The authors have the following interests: This study was partly funded by the Nichias Corporation. There are no patents, products in development or marketed products to declare. This does not alter the authors' adherence to all the PLOS ONE policies on sharing data and materials, as detailed online in the guide for authors.

* E-mail: mtagawa@chiba-cc.jp

Introduction

Malignant mesothelioma, often linked with asbestos exposure, evokes serious social concerns in many countries, and the patient numbers in Western countries and newly industrializing economies will progressively increase in the next decades [1,2]. Mesothelioma spreads along the pleural cavity and is often resistant to conventional treatments. Extrapleural pneumonectomy is applicable to the cases only at the early phase, but the recurrence is common despite the radical operation procedures. The current therapeutic strategy for the majority of mesothelioma cases is primarily chemotherapy, and a combinatory use of cisplatin (CDDP) and pemetrexed (PEM) is the first-line regimen [3]. A median survival period with the regimen is however relatively short, about 12 months, and possible second-line anti-cancer agents have not yet been demonstrated.

Mesothelioma has an unusual molecular lesion linked with loss of tumor suppressor functions. The majority of mesothelioma has a deletion in the INK4A/ARF locus which encodes the $p14^{ARF}$ and the $p16^{INK4A}$ genes, but possesses the wild-type *p53* gene [4]. Deletion of $p16^{INK4A}$ increases cyclin-

dependent kinase 4/6 activities, which subsequently induces pRb phosphorylation and cell cycle progression. In contrast, deficiency of $p14^{ARF}$ augments Mdm2 activities and consequently down-regulates p53 expression, which may render mesothelioma cells resistant to chemotherapeutic agents. Enhanced expression of p53 in mesothelioma is therefore a possible therapeutic strategy by inducing cell cycle arrest and apoptosis [5].

Interferons (IFNs) have anti-tumor effects by stimulating cell death and enforcing host immune systems. Three classes of IFNs have been identified, type I, II and III. Both type I and type III IFNs share similar biological activities including apoptosis induction, whereas type II IFN, IFN-γ, is primarily immune-stimulatory [6,7]. Type I IFNs, IFN-α and IFN-β, were well studied for the biological activities, and IFN-α but not IFN-β has been mainly tested for the anti-tumor actions in combination with anti-cancer agents in clinical settings. In contrast, type III IFNs, IFN-λs, have not been clinically tested for malignance and the precise mechanisms of type III IFNs-mediated apoptosis are not analyzed well [7,8]. As for mesothelioma, type I IFNs have not been rigorously studied for the therapeutic efficacy. There are only a few clinical studies on anti-tumor actions of IFN-α in combination with anti-cancer agents for mesothelioma [9–11], and combinatory effects of type I IFNs and PEM have not been examined. Recently, adenoviruses expressing the *IFN-β* gene were examined for the anti-tumor effects on mesothelioma in an animal model, and were clinically investigated for the safety and the therapeutic feasibility in mesothelioma patients [12,13]. Nevertheless, anti-tumor effects of recombinant type I IFNs in mesothelioma cells have not well studies particularly in terms of combination with the first-line chemotherapeutic agents. Moreover, differential biological activities between IFN-α and -β on mesothelioma remains uncharacterized.

A precise mechanism of IFN-mediated cell death also is unclear but Takaoka et al. demonstrated that type I IFNs up-regulated expression of the *p53* gene, suggesting a possible role of p53 in the type I IFN-mediated anti-tumor effects [14]. Nevertheless, type I IFNs produced apoptotic cell death even in *p53*-mutated tumors [15], which suggests p53 independent pathways in the IFNs-mediated cell death. In this study we compared anti-tumor effects of type I and type III IFNs with 5 kinds of *p53*-wild type mesothelioma cells, and investigated a possible up-regulation of p53 and combinatory effects of IFN with the first-line chemotherapeutic agents.

Materials and Methods

Cells

Human mesothelioma, NCI-H2452, NCI-H2052, NCI-H226, NCI-H28 and MSTO-211H cells, and mesothelium-derived Met-5A cells that were immortalized with the SV40 T antigen [16] were obtained from ATCC (Manassas, VA, USA). Human esophageal carcinoma T.Tn cells were from cell resource center for biomedical research, Tohoku University, Japan. They were cultured in RPMI-1640 medium supplemented with 10% fetal calf serum. All the mesothelioma cells used were defective of p14 and p16 expressions due to either loss of the transcription or deletion of the genomic DNA (Figure S1), and sequencing data confirmed that they possessed the wild-type *p53* gene.

Reverse transcription-polymerase chain reaction (RT-PCR)

First-strand cDNA was synthesized with Superscript III reverse transcriptase (Invitrogen, Carlsbad, CA) and amplification of equal amounts of the cDNA was performed with the following primers and conditions: for the *IFNAR-1* gene, 5'-CTTTCAAGTTCAGTGGCTCCACGC-3' (sense) and 5'-TCACAGGCGTGTTTCCAGACTG-3' (anti-sense), and 10 sec at 94 ˚C for denature/20 sec at 60 ˚C for annealing/32 cycles; for the *IFNAR-2* gene, 5'-GAAGGTGGTTAAGAACTGTGC-3' (sense) and 5'-CCC GCTGAATCCTTCTAGGACGG-3' (anti-sense), and 10 sec at 94 ˚C/20 sec at 56 ˚C/31 cycles; for the *IL-28Rα* gene, 5'-GGGAACCAAGGAGCTGCTATG-3' (sense) and 5'-TGGCACTGAGGCAGTGGTGTT-3' (anti-sense), and 10 sec at 94 ˚C/20 sec at 58 ˚C/31 cycles; for the *IL-10Rβ* gene, 5'-TATTGGACCCCCTGGAAT-3' (sense) and 5'-GTAAACGCACCACAGCAA-3' (anti-sense), and 10 sec at 94 ˚C/20 sec at 50 ˚C/32 cycles; for the *GAPDH* gene, 5'-ACCACAGTCCATGCCATCAC-3' (sense) and 5'-TCCACCACCCTGTTGCTGTA-3' (anti-sense), and 15 sec at 94 ˚C/15 sec at 60 ˚C/25 cycles.

Cell proliferation and viability test in vitro

Cells ($1x10^3$/well) were seeded in 96-well plates and were cultured with IFN-α2a (IFN-α), IFN-β1a (IFN-β) (PBL Interferon Source, Piscataway, NJ, USA) or IFN-λ1 (R&D Systems, Minneapolis, MN, USA) at different doses. In a combinatory treatment, cells were treated with various concentrations of CDDP or PEM and with IFNs. Cell viabilities were assessed with a WST kit (Dojindo, Kumamoto, Japan) which detected the amounts of formazan produced from the WST-8 (2-(2-methoxy-4-nitrophenyl)-3-(4-nitrophenyl)-5-(2,4-disulfophenyl)-2H-tetrazolium) reagent with the absorbance at 450 nm (WST assay). The relative viability was calculated based on the absorbance without any treatments. Combinatory effects were examined with CalcuSyn software (Biosoft, Cambridge, UK). Combination index (CI) values at respective fractions affected (Fa), which showed relative suppression levels of cell viability, were calculated based on the WST assay. CI<1, CI=1 and CI>1 indicate synergistic, additive and antagonistic actions, respectively. Viable cell numbers were counted with the trypan blue dye exclusion test. The statistical analysis was performed with one way analysis of variance (ANOVA).

Cell cycle analysis and cell surface staining

For cell cycle analysis, cells were fixed in ice-cold 70% ethanol, incubated with RNase (50 μg/ml) and stained with propidium iodide (PI) (50 μg/ml). For cell surface staining, cells were stained with fluorescein isothiocyanate (FITC)-conjugated anti-HLA-A, B,C antibody or FITC-conjugated isotype-matched control antibody (BD Biosciences, San Jose, CA, USA). The PI staining profiles and the FITC fluorescence intensity were